RÉPUBLIQUE ALGÉRIENNE DÉMOCRATIQUE ET POPULAIRE

MINISTÈRE DE L'ENSEIGNEMENT SUPÉRIEUR ET DE LA RECHERCHE SCIENTIFIQUE UNIIERSITÉ DE OUARGLA

FACULTE DES SCIENCES DE LA NATURE ET DE LA VIE ET SCIENCES DE LA TERRE ET DE L'UNIVERS DEPARTEMENT DE SCIENCES DE LA TERRE ET DE L'UNIVERS

Mémoire de Master Académique

Filière : Géologie

Spécialité : Géologie Pétrolier

Presented by: Kachi Boubekeur - Kherfi Bilal - Khazene Mohamed Lakhdar

Theme

Permeability estimation using flow zone indicator from Well log data of the oil field Northwest of Hassi Messaoud.

HACINI Massouad	**President**	**Professor**	**UKM Ouargla**
MEDJANI Fethi	**Examinateur**	**Professor**	**UKM Ouargla**
MEBROUKI Nassira	**Encadreur**	**MCB**	**ENSOuargla**

University : 2025/ 2026

Dédicaces

I can only thank God for this blessing that came after years of hard work, dedication, and patience. I would like to express my deepest love and gratitude to my mother and father, my true support and endless source of prayers, because without you I would never have reached this moment I had always dreamed of. I would also like to give special thanks to my dear aunt, who has always been a source of support, kindness, and encouragement, and to my cousin, who shared many beautiful moments with me and was the best companion throughout this journey. I will never forget my friends who stood by me every step of the way, easing the hardships and sharing hope and happiness with me. My sincere appreciation also goes to all my respected teachers, from primary school to university, who planted in us the values of knowledge, confidence, and ambition. This graduation is not only my achievement, but the result of all your love and support.

Kachi boubekeur

Dédicaces

I dedicate this modest work to my dear parents for their love, sacrifices, and unwavering support throughout my university journey. May they find here the expression of my deep gratitude and immense appreciation.

I also dedicate it to my brothers and sisters for their constant encouragement, affection, and precious presence during difficult times.

My sincere thanks also go to all my friends and colleagues who supported, advised, and accompanied me throughout this academic adventure.

Finally, I dedicate this dissertation to all those who contributed, directly or indirectly, to the completion of this work.

Khazen Mohamed Lakhdar

Dédicaces

In the Name of Allah, the Most Gracious, the Most Merciful

All praise is due to Allah, who granted me the strength, patience, and guidance to complete this modest work.

I dedicate this achievement to my beloved parents, whose endless love, sacrifices, and support have been the foundation of my success. May Allah bless them and reward them abundantly.

To my brothers and sisters, for their encouragement, understanding, and constant presence throughout my academic journey.

To my esteemed teachers and professors, who generously shared their knowledge and guided me toward learning and excellence.

To my friends and colleagues, who accompanied me during this journey and provided motivation and support whenever needed.

To everyone who contributed, directly or indirectly, to the completion of this work.

I dedicate this humble achievement with sincere gratitude and appreciation, hoping that it will be beneficial and a source of pride

for all those who supported me.

Khrfi bilal

REMERCIEMENTS

في البداية، نحمد الله تعالى الرحمان الرحيم الذي منحنا القوة والصبر لإتمام هذا العمل المتواضع.

نتقدم بخالص الشكر والتقدير إلى مشرفتنا الدكتورة مبروكي نصيرة على تفرغها لنا، وجديتها، وتوجيهاتها القيّمة.

كما نتوجه بالشكر الجزيل إلى جميع أعضاء لجنة المناقشة الذين شرفونا بقبول تقييم ومناقشة هذا العمل.

وبهذه المناسبة، نتقدم بالشكر أيضًا إلى جميع أساتذة قسم علوم الأرض والكون بجامعة ورقلة، وإلى كافة الطاقم الإداري، بعد مسيرة دامت خمس سنوات حافلة بالذكريات الجميلة.

كما نعبر عن أسمى عبارات الشكر والامتنان للسيدة مبروكي نصيرة على مساعدتها لنا وتخصيصها. جزءًا كبيرًا من وقتها الثمين للمساهمة في إنجاز هذا العمل.

وفي الأخير، نتوجه بالشكر إلى كل من ساهم من قريب أو بعيد في إنجاز هذا العمل وإتمامه.

يرتكز الإطار الجيولوجي على تكوين Ra الكمبري ــــ الخزان الرئيسي للحقل ــــ المقسَّم إلى خمس وحدات فرعية (D1 إلى D5)، مؤلَّفة من حجر رملي كوارتزي متفاوت الحبيبات على أعماق تتراوح بين 3345 و3520 متراً. كشف التحليل البتروغرافي عن أربعة متباينات دقيقة: أرينابيت كوارتزية صوّانية، وأرينابيت كوارتزية كاولينيتية-صوّانية، وأرينابيت كوارتزية ميكائية-كاولينيتية-صوّانية، وسابركوز ميكائية-طينية. تُفسد العمليات الديجنيتية ــــ الانضغاط والإسمنت السيليسي والكالسيتي ونمو المعادن الطينية ــــ جودة الخزان، في حين يُسهم التشقق والإذابة في استعادة جزء من هذه الجودة.

احتُسب FZI في خمسة آبار (OMJ24، OMJ41، OMJ223، OMK25، OMK142) عبر معلمات تسجيل محوَّلة. تكشف النتائج عن تغاير واضح بين الآبار: يُسجِّل البئر OMJ024 جودة خزان ممتازة في وحدة D5؛ ويحدد البئر OMJ041 فترات حاملة للهيدروكربونات عند عمق 3477 متراً؛ ويُظهر البئر OMJ223 قيم FZI مستقرة تدل على تجانس جيولوجي ملائم للإنتاج؛ فيما يعكس البئر OMK142 تراجعاً في الكفاءة الهيدروليكية بسبب ارتفاع محتوى الأرجيل.

تُثبت الدراسة أن FZI أداة موثوقة لتصنيف وحدات التدفق الهيدروليكي (HFU) والتنبؤ بالنفاذية في الفترات غير المستخرجة، وتوصي بدمجه مع بيانات تسجيل الإنتاج لتحسين إدارة الخزانات.

The geological setting is anchored in the Cambrian Ra formation — the field's primary reservoir — subdivided into five sub-units (D1 through D5), composed of poorly sorted quartzose sandstones at depths between 3,345 and 3,520 m. Four microfacies were identified petrographically: siliceous quartz arenite, kaolinitic-siliceous quartz arenite, micaceous-kaolinitic-siliceous quartz arenite, and micaceous-argillaceous subarkose. Diagenetic processes — compaction, silica/calcite cementation, and clay mineral authigenesis — degrade reservoir quality, while fracturing and dissolution partially restore it.

FZI was computed across five wells (OMJ24, OMJ41, OMJ223, OMK25, OMK142) using transformed log parameters. Results confirm high inter-well heterogeneity: well OMJ024 shows excellent reservoir quality in the D5 unit; well OMJ041 identifies hydrocarbon-bearing intervals at 3,477 m; well OMJ223 exhibits stable FZI values indicating geological homogeneity favorable to production; well OMK142 reflects degraded hydraulic efficiency due to shale content.

The study validates FZI as a reliable tool for Hydraulic Flow Unit (HFU) classification and permeability prediction in uncored intervals, recommending integration with production logging data for enhanced reservoir management.

Abstract

Table des matières

List of figures

Introduction Genral

Oil and gas play a crucial role in the industries of many countries. Extracting these resources from the subsoil demands significant investment and extensive, complementary, and successive operations. In Algeria, one of the world's largest oil producers, companies like Sonatrach are pivotal in this process.

Algeria is the largest country in Africa and the Arab world, covering 2, 381,741 km². Its natural boundaries include the Mediterranean Sea to the north with 1,200 km of coastline, Morocco to the west, Mauritania and Western Sahara to the southwest, Mali and Niger to the south, and Tunisia and Libya to the east.

Algeria's landscape is divided into four regions from north to south :

The Tellian Atlas, featuring steep reliefs and coastal plains, with the richest areas being Mitidja in the center, Chelif in the west, and Seybouse in the east.

The Saharan Atlas, a series of NE-SW oriented reliefs extending from the Moroccan border to Tunisia.

The Sahara, containing the majority of hydrocarbon resources, characterized by large dunes (East and West Ergs), rocky plains (regs), and oases with increasing urbanization.

The Eglab Mountains to the southwest and the Hoggar Mountains to the south.

Structurally, Algeria is divided into two major tectonic units by the Atlasic south fault :

The northern alpine area, marked by mountain ranges from the tertiary period due to alpine orogenesis.

The southern Saharan shelf, a more stable area with a Precambrian bedrock overlaid by thick sedimentary series deposited in basins primarily structured during the Paleozoic.

Algeria has three oil provinces : north, west, and east.

The northern province includes the basins of South-East Constantinois–Melrhir, Hodna, Chelif, Offshore, and Saharan Atlas.

The western province includes the basins of Ahnet, Timimoun, Béchar-Oued Namous, Reggane, Tindouf, Taoudeni, and Sbâa.

The eastern province includes the basins of Illizi, Berkine, Oued Mya, and the mole Amguid-Messaoud, which contains the giant Hassi Messaoud (oil) and Hassi R'mel (gas) fields where most oil and gas discoveries have been made to date.

The Hassi Messaoud field, one of the largest and most complex reservoirs globally, was discovered on January 16, 1956, by SN-REPAL through the first drilling (MD1) following a seismic refraction campaign on June 15, 1956. This 3,338m deep drilling revealed oil producers from the Cambrian age.

Over geological history, the Hassi Messaoud deposit experienced significant tectonic evolution, shaping its current form and influencing its characteristics. Studying the reservoir is the most important phase in oil exploitation as it provides insight into the hydrocarbon deposit. This study employs behavior analysis techniques for better data acquisition, optimizing hydrocarbon recovery within an economic framework aimed at developing the field.

Our study focuses on the northwest part of the Hassi Messaoud field. In this study, we tries to shed light on the Petrography and petrophysical characteristics of the Cambrian reservoirs, in the north western of Hassi messaoud Field, The hydraulic flow unit (HFU) approach has been used for classification of rock types and prediction of flow properties, as an integrating tool for petrophysical description of the reservoir. Development and application of the HFU approach is stimulated by the common problem of permeability prediction in uncored but logged wells (Svirsky et al., 2004). Classical approaches for estimation of permeability are based either on simple logarithmic regressions evaluating permeability from log-derived porosity (Eq. 1) or on empirical correlations which relate permeability to various log responses. $\ln K = a.\square + b$………………………… (1) a and b are constants.

The hydraulic unit is defined as the representativeelementary volume of total reservoir rock withinwhich geological and petrophysical properties thatcontrol fluid flow are internally consistent andpredictably different from properties of otherrocks (Amaefule et al., 1993). The fundamentalpetrophysical units in a reservoir (rock types) can be determined by flow zone indicators for routinecore plug analysis. The variation in thepetrophysical properties (porosity & permeability).(Tanmay Chandra,2008)

should be small for a given rock type implyingthat knowledge of any porosity or permeabilitywill enhance the prediction of the other properties.This technique of calculating FZI from core datahas been introduced by Amaefule et al., 1993,which involves normalized porosity index (NPI)and reservoir quality index (RQI) throughequation 2.

Flow Zone Indicator (FZI): Flow Zone Indicatoris a unique and useful value to quantify the flowcharacter of a reservoir and one that offers arelationship between petrophysical properties atsmall-scale, such as core plugs, and large-scale,such as well bore level. In addition, the term ofFZI provides the representation of the flow zonesbased on the surface area and tortuosity. It ismathematically represented as (Al-Dhafeeri et al,2007)

$FZI = RQI / NPI = \{(.0314\sqrt{K/\Phi})\} / \{\Phi / (1- \Phi)\}$…... (2)

Where,FZI=Flow Zone Indicator, μm.

K=Permeability, md.

Φ=Porosity, volume fraction.

Chapter 01: Geologic setting

1. Introduction

Hassi Messaoud is located 800 km south of Algiers, between the meridians 5°30 and 6°00 and the parallels 31°00 and 32°00N. This Hassi Messaoud field is 350km from the Algerian-Tunisian border and 80km from the city of Ouargla. (Figure 01)

It has an area of 2000Km², at an altitude of 142m. The climate is desert with temperatures ranging from 0°C to 47°C on average. (Sonatrach document)

Had been granted to the company SN REPAL (National Company of Petroleum Research in Algeria) and the company CFPA (The French Petroleum Company in Algeria) its Lambert coordinates are:

X= 790,000 - 840,000 East.

Y= 110,000 - 150,000 North.

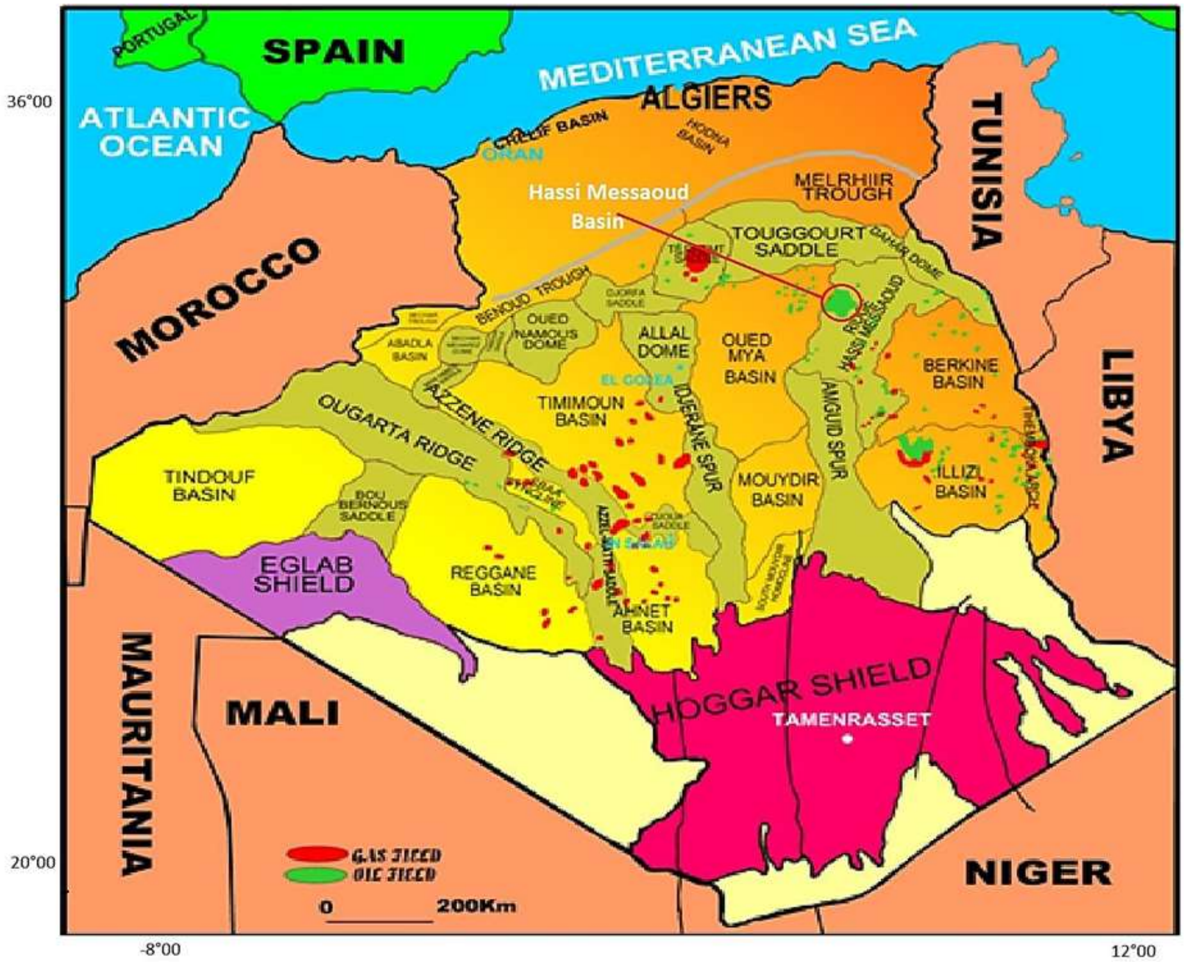

Figure 1.01 : The main Algerian sedimentary basins. Hassi Messaoud Basin is surrounded by a red circle. (Sonatrach document and NassiraMebrouki el al.2024)

2. Hassi Messaoud field

2.1. Geological situation

The Hassi Messaoud deposit is located within the Triassic platform, on the Amguid shoal; it is geologically limited; to the north by the Djamâa-Touggourt structure, to the south by the mole of Amguid El Biod, to the east by the shoals of Dahar, Rhourde El Baguel and the depression of Ghadames and to the west by the depression of Oued -Mya.(Source : Sonatrach document) (Figure 02).

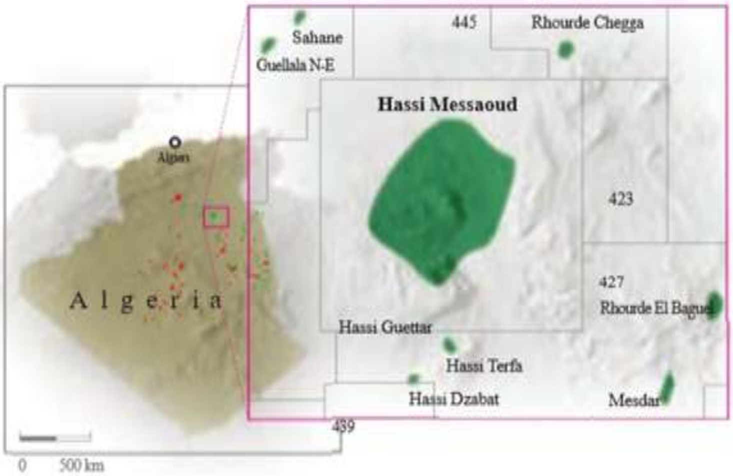

Figure 1.2: Location of the Hassi Messaoud field. (Hydrocarbon Reservoirs of Algeria, WEC 2007)

2.2. Zoning of the Hassi Messaoud field

The evolution of well pressures relative to production has led to the subdivision of the Hassi Messaoud deposit into 25 production zones of varying extents. These zones are relatively autonomous, comprising a network of wells that communicate internally but not with neighboring zones. Each zone exhibits specific reservoir pressure behaviors. Wells within the same zone collectively extract a predetermined volume of oil in situ. However, it's crucial to emphasize that pressure alone cannot serve as the sole criterion for characterizing these areas.

2.3. Well number

The Hassi Messaoud field is divided into two distinct parts: the North zone and the South zone, each having its own numbering established by the first detecting companies of the field.

North field: includes a geographic numbering supplemented by a chronological numbering, example: Omn 63.

O: Capital letter, Ouargla permit., m: Tiny, 1600 Km2 tile, n: Tiny, square of 100 Km2

6: X-axis, and 3: Y-axis

South field: It is mainly chronological supplemented by a geographical numbering based on abscissas and ordinates of interval equal to 1,250 Km and harmonized with the lambert coordinates Ex: Md10.

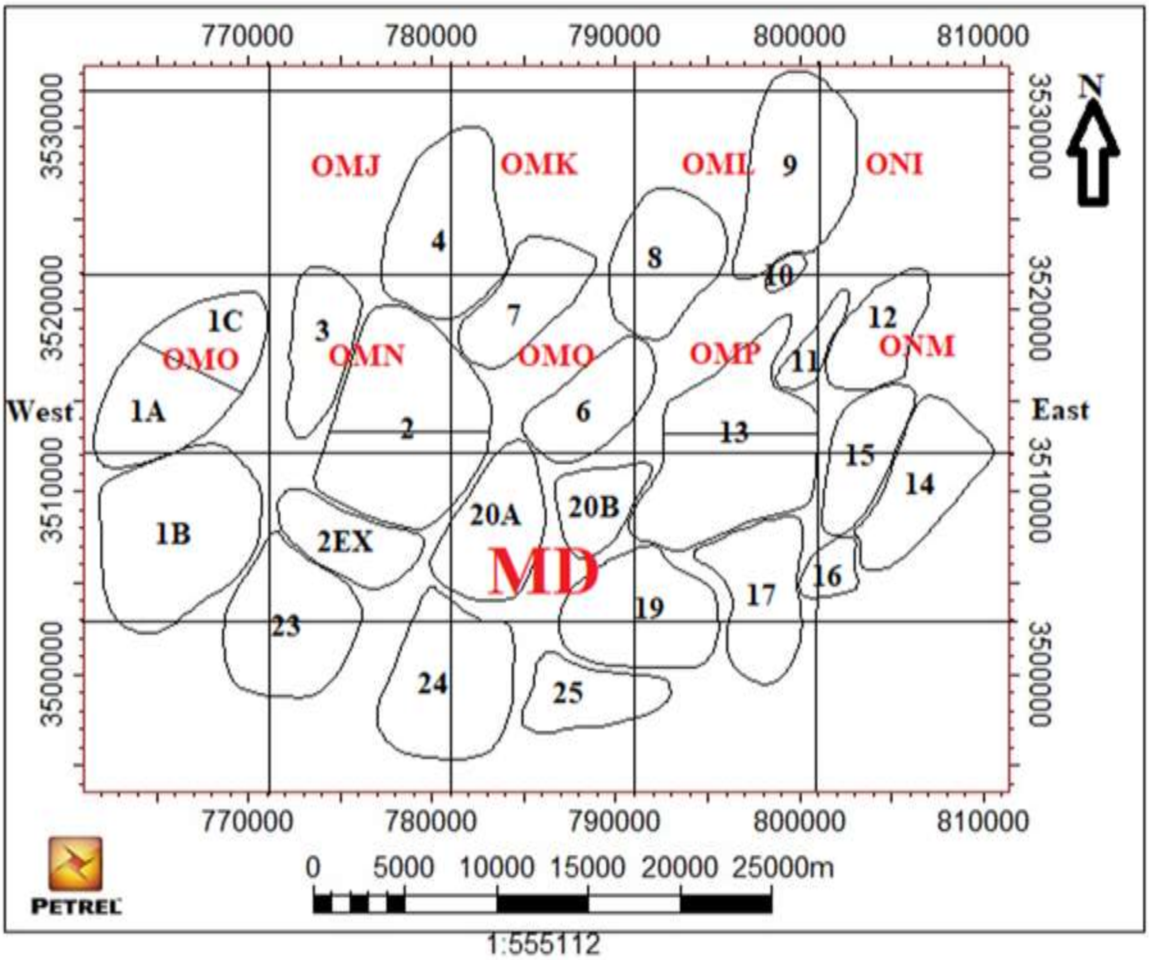

Figure 1.3:: Different sectors within the Hassi Messaoud Field are identified by initial letters, which are used to name the producing wells and indicate their location within the field.(Nassira Mebrouki el al. 2024)

3. Stratigrphy

A revised generalized stratigraphic section of the Hassi Messaoud ridge (Figure 04) delineates the various rock units commonly encountered in the region. This depiction draws from the research of Balducchi and Pommier (1970), De Lapparent (1961), and Malenfer and Tillous (1963), as referenced by Djamel Boutoutaou in 2003.

3.1. Prehercynian sedimentary cycle

3. 1.1. Paleozoic (Figure 04)

3.1.1.1. Cambrian

Malenfer and Tillous (1963) categorized the Cambrian sediments in the Hassi Messaoud field into five principal units: Zone R3, Zone R2, Zone Anisometrique (Ra), Zone

Isometrique (Ri), and Zone des Alterances. Among these, Ra serves as the primary reservoir unit, while Ri and R2 are considered secondary reservoirs. This classification draws from various published works by Balducchi and Pommier (1970), Bacheller and Peterson (1991), and Fennouh (1996).

Zone R3, or Cambrian unit R3, comprises highly cross-bedded, arkosic, and quartzose sandstone with notable clay content, primarily illite. It contains approximately 60% quartz and 30% clay, with a basal conglomerate of pebbles to cobbles. Thickness varies from 275 meters to 368 meters across the field, believed to have originated from moraines and tillites deposited during the Eco-Cambrian period and subsequently redistributed by alluvial streams.

The Cambrian unit R2, also referred to as zone R2, comprises a substantial sequence of sandstones characterized by a high clay content. These sandstones exhibit a medium to coarse-grained texture and contain interstitial clay with occasional thin inter-beds of shale. Predominantly composed of illite with some kaolinite, the presence of clays renders the reservoir quality of this zone poor, leading to its general non-productivity. However, in the northeastern sector of the field, the upper 20 meters of this zone are considered part of the productive interval. In areas unaffected by erosion, the thickness of zone R2 can reach up to 80 meters.

The Cambrian unit Ra, also known as the Zone Anisometrique, constitutes a significant reservoir in the Hassi Messaoud field. In its pristine state, it boasts a maximum total thickness of 150 meters in the western sector, unaffected by erosion cycles. Ra is further subdivided into five sub-zones: Drain 4, Drain 3, Drain 2, Inter-drain, and Drain 1. These sub-zones share similar lithological attributes, primarily comprising highly cross-bedded, very poorly sorted, medium-grained to micro-conglomeratic quartzose sandstones. Interdispersed within these sandstones are irregular lenses of shaly siltstone. Quartz predominates in the Ra zone, accounting for approximately 70% of its composition, while secondary silica and clay make up around 14% and 8%, respectively. In certain wells, kaolinite serves as the primary clay mineral. Drain 3, known as the "Median Zone," stands out for its finer-grained texture and lack of cross-bedding. Noteworthy for its abundant tubular fossils called scolites, Drain 3 primarily comprises kaolinite. Studies by L'Homer (1967) and Beuf et al. (1971) suggest that the Ra sediments were deposited in alluvial fan and associated depositional environments. Despite variations in Drain 3, the thickness and continuity of the sub-zones remain remarkably consistent throughout the field.

The Cambrian Ri, also identified as Zone Isometrique, represents a quartzitic sandstone unit approximately 50 meters thick. It exhibits a uniform thickness, comprising well-sorted, medium-grained sandstone interspersed with interbeds of shale and silstone. Throughout its extent, Ri contains numerous tubular fossils referred to as scolites, except for the basal meter, which comprises winnowed debris from the underlying formation. Overlying the Ra zone unconformably, the contact between Ri and Ra corresponds to L'Homer's (1967) "Gamma Zero" marker in fieldwide correlations. Despite containing hydrocarbons when above the oil-water contact, RI is not considered a significant producing zone due to its poor reservoir characteristics. Nevertheless, the top of Ri still marks the top of the reservoir section.

The Zone Alternances comprises alternating layers of quartzites, siltstones, and black shales, ranging from 25 to 40 meters in thickness. It is commonly recognized as the lowermost part of the Ordovician sequence according to previous studies.

3.1.1.2. The Ordovician

The Ordovician is a geological period that is characterized by the presence of various rock formations in the Hassi Messaoud field. These formations are eroded over a large area but are still present in the immediate vicinity of the field. Some of these formations are also found within the field boundary, particularly in the narrow grabens in the southern part of the field and the northeast sector. The Ordovician section in this area includes the following formations: El Azzel Shales Formation, Ouargla Sandstones Formation, Hamra quartzite Formation, El Atchane Sandstones Formation, and El Gassi Shales Formation. These formations vary in composition and reservoir quality, with some being fine-grained quartzite with low porosity and permeability, while others are black glauconitic, graptolitic marine shale

3.2. Post hercynian sedimentary cycle

3.2.1. Mesozoic

3.2.1.1. Triassic

The Triassic is characterized by the deposition of sedimentary rocks that are divided into two units: the Upper Triassic and the Lower Triassic. The Upper Triassic is composed mainly of massive anhydrite and halite, while the Lower Triassic consists of a basal clastic section. The thickness of the basal unit can vary greatly due to the irregular erosion surface upon which it was deposited, with topography reaching up to 30 meters. (Figure 04)

3.2.1.2. The Jurassic

The Jurassic period is characterized by a thick sequence of rock layers (850 m thick), with the upper third consisting of massive dolomite. This dolomite is separated from the underlying massive salt and anhydrite unit by a thick shale section known as the Dogger Lagunar.

3.2.1.3. The Cretaceous

The Cretaceous period is characterized by the presence of various sedimentary rocks such as anhydrite, halite, limestone, and dolomite. These rocks are found in the upper 800 meters of the Cretaceous section. Additionally, the lower Cretaceous is composed of a thick clastic unit consisting of siltstone, shale, and fine-grained sandstone, spanning a thickness of 850 meters. Within this lower unit, there is a prominent dolomite bed that is approximately 25 meters thick.

3.2.1.4. The Miocene-Pliocene

The Miocene-Pliocene period is characterized by the presence of approximately 250 meters of sand, sandstone, and sandy shale sediments.

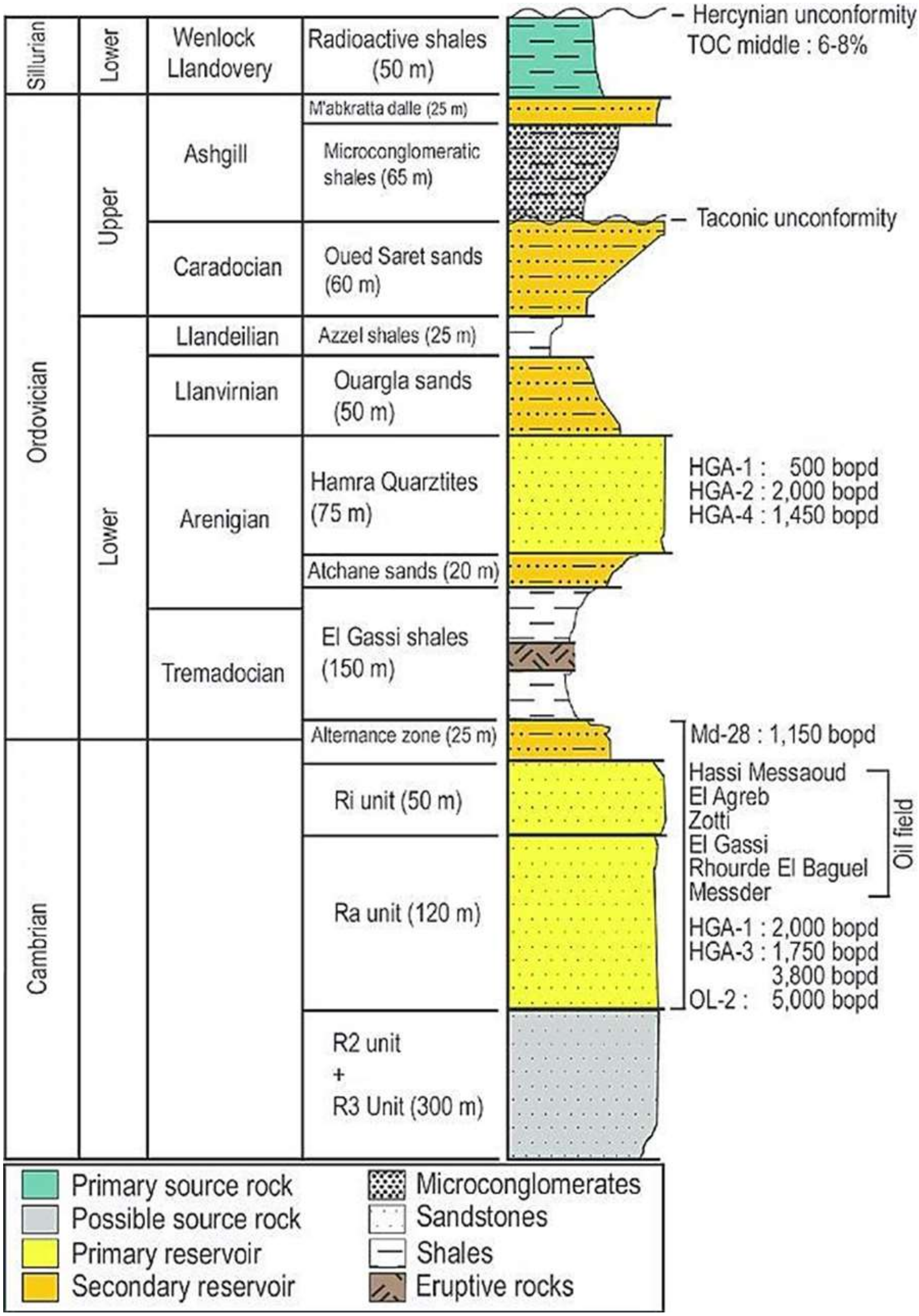

Figure 1.4:: The stratigraphic column of the Paleozoic sequence in Hassi Messaoud Field, Algeria (Zerroug et al., 2007; Aïfa et al., 2014).

1. Depositional environments and diagenesis

The depositional environments in the studied area consist of a complex system of braided river channels in the lower R3, R2, and Ra units. These units are overlain by finer sandstones with skolithos and clayey siltstone levels in the upper Ra, indicating a shallow marine environment. The marine episode continued into the Ordovician, with the deposition of fine sandstones containing skolithos and clays. The sandstones in reservoirs Ri and Ra, as well as the Hamra quartzites, often exhibit a predominance of silica, with kaolinite being the main clay mineral. Secondary silica growth is observed in fault zones and as a fill for faults and fractures. The sandstones in reservoirs R2 and R3 show a higher volume of detrital or authigenic illite compared to silica. (Hydrocarbon Reservoirs of Algeria, WEC2007)

2. Structure

The Hassi Messaoud field has a structure of an anticlinal dome, which was formed during the Hercynian orogeny. The field is extensively compartmentalized by regional fault systems and complex perpendicular and parallel systems on a smaller scale. The field is also characterized by deep narrow valleys filled with volcanic rocks, and the structural dip ranges from 4 to 10 degrees. The presence of fissures associated with the faults contributes to increased permeability and production. The volcanic rocks are mainly found in the southern part of the field. (Hydrocarbon Reservoirs of Algeria, WEC2007)

3. Tectonic

The tectonic environment of the Hassi Messaoud area on the Sahara platform has undergone significant deformation and tectonic activities over its geological timeline. During the deposition of Cambrian sandstones, a stable subsiding region prevailed with a northward paleo-current direction. However, towards the end of Ra formation deposition, there was a brief episode of activity in the Hassi Messaoud structure, resulting in erosion of approximately 50 meters of that unit. Evidence of the Hercynian orogeny is widespread, manifested by extensive faulting and deep erosion in the Cambrian and Ordovician rocks. These tectonic events and erosion persisted from the Late Devonian through the end of the Permian era, ultimately giving rise to the Hassi Messaoud - El Agreb anticlinorium. Following the final phase of the Hercynian orogeny, Triassic sediments were deposited alongside the extrusion of Triassic igneous rocks. Subsidence of the Sahara platform occurred gradually from the pre-Late Triassic period to the conclusion of the Cretaceous, accumulating evaporite and elastic sediments. The absence of early Tertiary rocks suggests uplift along the Hassi Messaoud - El Agreb high. Since then, the area has remained tectonically quiescent, characterized by the presence of flat-lying continental Miocene-Pliocene rocks.

4 Petroleum system

4.1. Source rocks

The primary source rock in the Amguid - Hassi Messaoud basin is the Silurian (Figure 05), characterized by radioactive gray-black to black clays abundant in organic material. This source rock predominantly yields gas in the western areas, whereas in the eastern region, oil generation occurred during the late Jurassic and early Cretaceous epochs. The oil derived from the Silurian source rock has significantly contributed to the region's reserves, estimated at approximately 1.08 billion barrels of oil and 730 trillion cubic feet of gas. Remaining undiscovered oil reserves in the area are projected to be around 48 billion barrels, primarily situated in the Cambro-Ordovician plays to the northwest of the Berkine, and the Triassic plays in the northern and western sectors of the Hassi Messaoud dome.

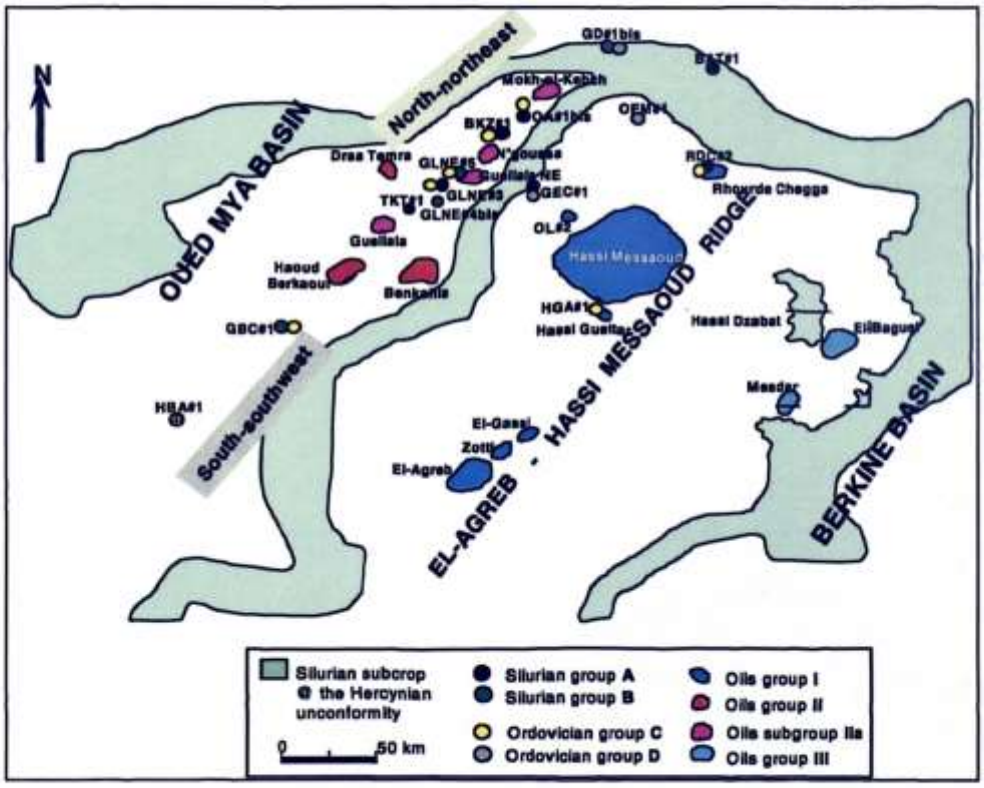

Figure 1.5: Silurian, Ordovician source rock samples and oil fields location map. (Djamel Boutoutaou, 2003)

4.2.Seal Rocks

The Amguid – Hassi Messaoud uplift has multiple layers of rock seal that vary in age and type. The El Gassi clays cover the Cambrian reservoirs, while the Azzel clays seal the Hamra quartzites reservoir in the Ordovician. The most effective seals are the clay-evaporite deposits of the Triassic and Liassic.

4.3.Reservoirs Rocks

The Cambro-Ordovician reservoir has been drilled across several structures but has displayed only restricted oil accumulations. Nonetheless, the Hamra quartzites within this Ordovician reservoir have exhibited notable oil saturation, boasting columns exceeding 100 meters in height and surface areas surpassing 500 square kilometers. Test results have revealed oil flow rates ranging from 6 to 14 cubic meters per hour. The distinctive ring-like configuration of the Ordovician reservoir further elevates its attractiveness.

The Cambrian formation in Hassi Messaoud and its vicinity serves as a productive reservoir across multiple fields. Within the Cambrian play, the Ri unit acts as a transitional layer between different facies. It comprises medium to coarse sandstones with bioturbation. At the top of the Ri reservoir lies a shallow marine sandstone, rich in bioturbation. The thickness of the Ri reservoir can fluctuate, and it may also show unconformity with the Ra reservoir.

The Ordovician era is marked by the presence of the Taconian unconformity, which acts as a boundary between the basal Ordovician and the Upper Ordovician. This unconformity comprises fluvio-glacial and glacio-marine formations. The lower Ordovician is characterized by two transgressive-regressive cycles, featuring formations deposited in shallow to fluviatile marine environments. The Middle Arenigian-Caradocian cycle encompasses various rock formations and is occasionally truncated by the Taconian unconformity in specific regions, including the Hamra quartzites, Ouargla sandstones, Azzel marine clays, and the Oued Saret littoral deltaic sandstones

Triassic is characterized by challenges in petrographic and petrophysical characterization due to lateral discontinuity in sandstone bodies and compaction related to diagenetic phenomena. The deposits are concentrated in NE-SW oriented depressions and are marked by evaporitic formations, volcano-detritic deposits, and lagoonal deposits. The facies of the basin vary depending on the location of sedimentation and distance from input sources. The deposits are generally continental at the base and become more evaporitic towards the top.

4.4.Traps

Exploration efforts have primarily focused on structural and mixed traps, with a particular emphasis on stratigraphic traps. Structural traps in the Middle Triassic are typically anticlinal folds that formed during different tectonic phases, either as a result of fracturing tectonics or bounded by major faults within the complex Amguid Hassi Messaoud High system. Stratigraphic traps, on the other hand, involve sandstone bodies that have been closed off by lateral wedging.

7. Lithological description of the reservoirs

7.1. The Cambrian reservoir

The Cambrian Ri/Ra lithology consists of a thick sequence of detritic rocks, including sandstones, quartzites, and conglomerates. The lower member, Ra, is composed of fine to coarse gray-white sandstones and compact light-gray conglomerates. The upper member, Ri, is characterized by pinkish gray sandstones of quartzite composition with a siliceous cement. The sandstone bodies and silts of reservoir Ra are discontinuous and of small lateral extent, while sandstone Ri shows better continuity.

7.2. The Ordovician reservoir

The Ordovician lithology consists of a 90-meter thick formation characterized as massive and compact. It is composed of fine to medium, locally coarse, compact hard silico-quartzite to quartzite, white to gray-white sandstone with episodes of black, silty, laminated clay. Different lithofacies have been identified, including horizontally bedded fine to very fine quartzite sandstone, obliquely bedded very fine to fine quartzite sandstone, bioturbated very fine to fine quartzite sandstone, crossbedded very fine to fine quartzite sandstone with graded bedding, very fine to fine sandstone with clay chips, clay pebbles, and clay films, and very fine to fine quartzite sandstone. The presence of ichnofacies associated with Scolithus indicates an upper shoreface, marine-type environment.

Introduction

Core analysis provides essential information that cannot be obtained from wireline log measurements or drill cutting samples. The sedimentological data derived from a core far exceed the information provided by wireline logs and cutting samples. This includes detailed lithology and both macroscopic and microscopic definitions of the heterogeneities in the reservoir rocks, as well as fundamental reservoir data. Core data are also used to calibrate log responses (Miall, 1984).

In this study, conventional cores from nine wells (see Figure) were analyzed. These cores were examined, described, and photographed, with further core analysis and thin section studies conducted on these samples.

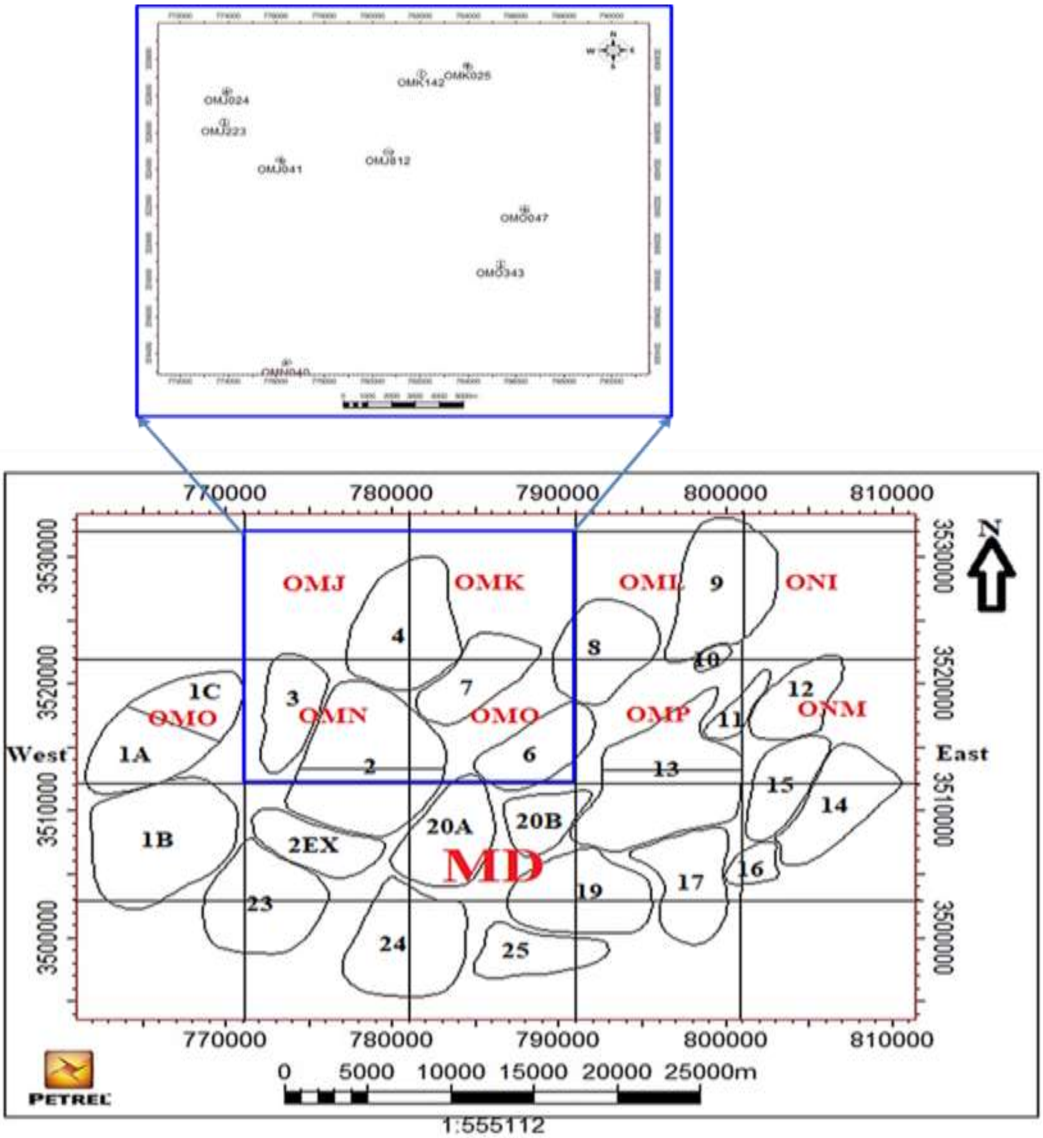

Figure 3.1: Position of the study wells northwest of the Hassi Messaoud (Nassira Mebrouki, Messaoud Hacini and al, 2024)

Chapter 02: Methodology

1. Methods and Available Data

1.1. FZI (Flow Zone Indicator)

To obtain FZI (Flow Zone Indicator) for uncored interval / well, the various log parameters such as GR (gamma Ray), ϕn (neutron porosity), ρb (density), Rt true resistivity) are obtained for depth intervals: 657 plugs from 3405-3487 m loged interval of **OMJ24**,889 plugs from 3367-3478 m loged interval of **OMJ41**,1077 plugs from 3385-3519.5 m loged interval of **OMJ223,**577 plugs from 3345-3417 m loged interval of **OMK25**,, 505 plugs from 3354-3417 m loged interval of **OMK142**(They are loged systematically each 25 cm of the cored intervals of none wells) FZI is calculated for these selected porous and permeable depth intervals using a technique given by Xue and Dutta Gupta, 1997. This technique is based on the transformation of gamma ray (GR), neutron porosity (NPHI), density (RHOZ) and resistivity (LLD) logs as given below:

- GR_Tr = 4.7860E-03 GR2 – 1.7320E-01 GR + 1.0614E+00 ------------ (1)
- NPHI_Tr = -8.1102E+00 NPHI 2 + 9.6676E-01 NPHI + 1.7170E-01 --------- (2)
- RHOZ_Tr = 7.1926E+00 RHOZ 2 – 3.6727E+01 RHOZ + 4. 5873E+01 -------- (3)
- LLD_Tr = -1.6859E-04 HLLD 2 – 3.8016E-02 LLD + 4. 3712E-01 -------- (4)
- SUMTr = GR_Tr + NPHI_Tr +RHOZ_Tr + LLD_Tr --------------------- (5)
- FZI = 4.4306E-01 SUMTr2 + 6. 08575E-01 SUMTr + 3.8229E-01 -------------- (6)

SUMTr is the sum of all transform given by equations (1-4). Equation (6) gives the relation between the log motifs and FZI.

1.2. Petrography

For delineating the mineral composition, facies types, and the predominant diagenetic features, a total of 723 samples were slapped and impregnated with blue-dyed Araldite, then prepared as thin sections that were studied using a polarized microscope supported with a Pc monitor for imaging. (Nassira Mebrouki, Messaoud Hacini and al, 2024)

For more detailed petrographic investigations, Scanning Electron Microscopy (SEM) of magnification up to 100,000 times is applied to delineate the clay and authigenic mineral types, visualize the internal grain and pore fabrics and connectivity, fracturing, clogging types, and their spatial distribution. It is applied to 16 freshly broken samples coated with gold and adhered to aluminum strips. These samples were selected from the subsurface Cambrian sequence in OMJ24, OMJ223, OMJ41 and OMJ812 wells, and OMK25, and OMK142 wells in northwesternHassi Messaoud Field, East Algeria (figure). Image data were released by the Research and Development Center of Sonatrach Petroleum Corporation. (Nassira Mebrouki, Messaoud Hacini and al, 2024)

1.3. Integrating Petrography and FZI

The methodology adopted in this study relies on an integrative approach designed to correlate textural petrographic characteristics with reservoir hydraulic behavior. This framework involves calibrating the Hydraulic Flow Units (HFUs) derived from the Flow Zone Indicator (FZI) method with qualitative data obtained from detailed petrographic analysis (thin-section and SEM). This methodology enables the conversion of micro-scale rock descriptions—such as facies type, clay content, and diagenetic modifications—into quantitative parameters, thereby providing a robust physical basis for calibrating mathematical models used in permeability estimation. Consequently, this approach enhances the accuracy of reservoir property predictions in uncored intervals by grounding hydraulic behavior within the geological reality of the rock system.

Chapter 03 :Permeability estimation using flow zone indicator from Well log data

1. Flow Zone Indicator (FZI)

This study relied on the Flow Zone Indicator (FZI) to characterize petroleum reservoirs and evaluate their hydraulic properties using wireline log data. The main objective was to divide the reservoir into homogeneous Hydraulic Flow Units (HFUs) and improve permeability estimation in uncored intervals, following the methodology proposed by Amaefule et al. (1993).

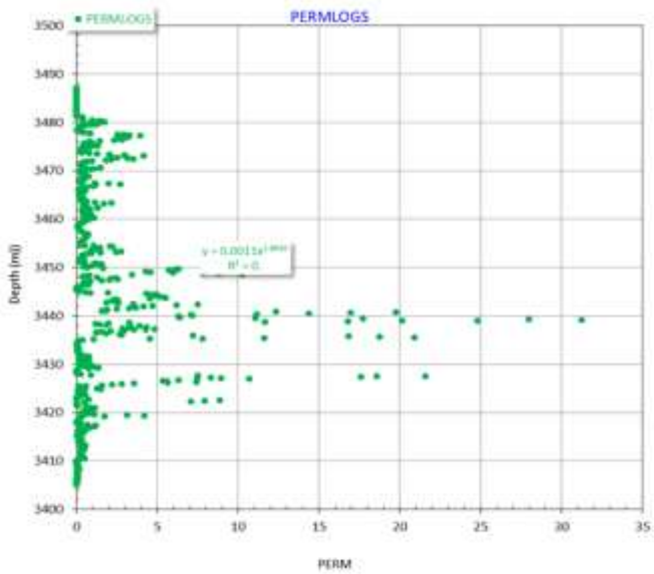

Permeability Vs Depth plot for well OMJ24

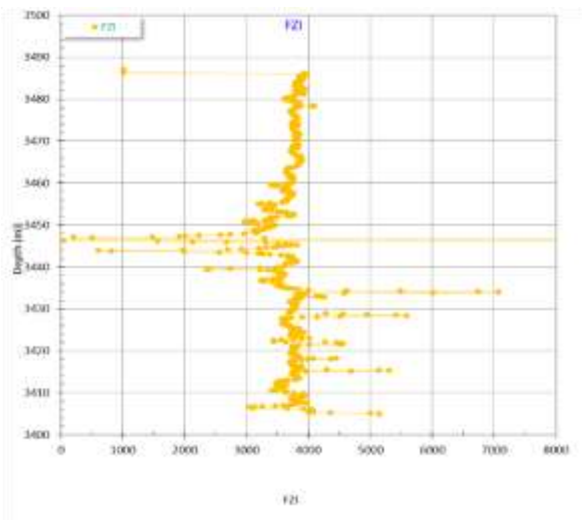

FZI vs. Depth plot for well OMJ24

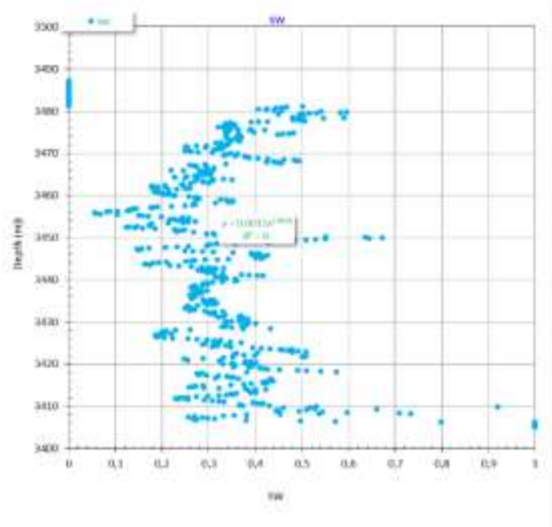

Water Saturation Vs Depth plot for well OMJ24

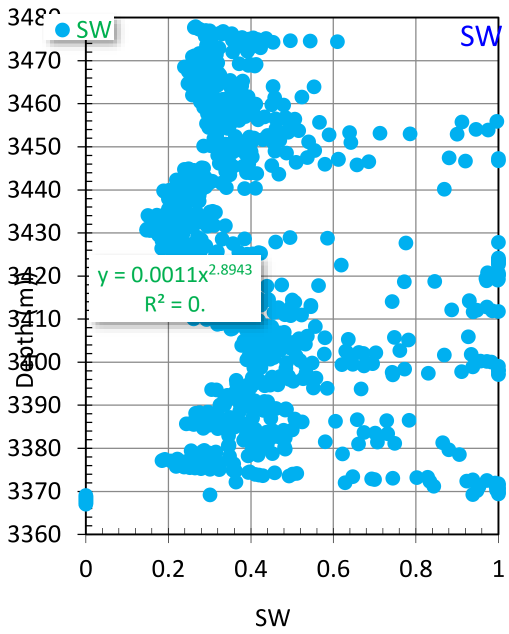

Water Saturation Vs Depth plot for well OMJ41

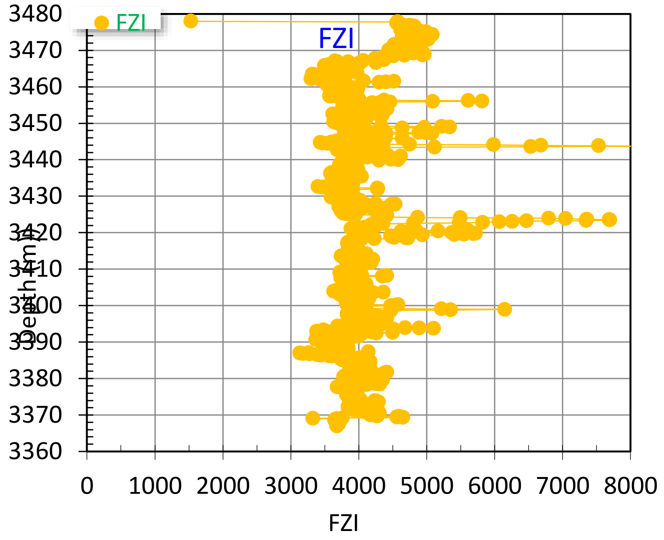

FZI vs. Depth plot for well OMJ41

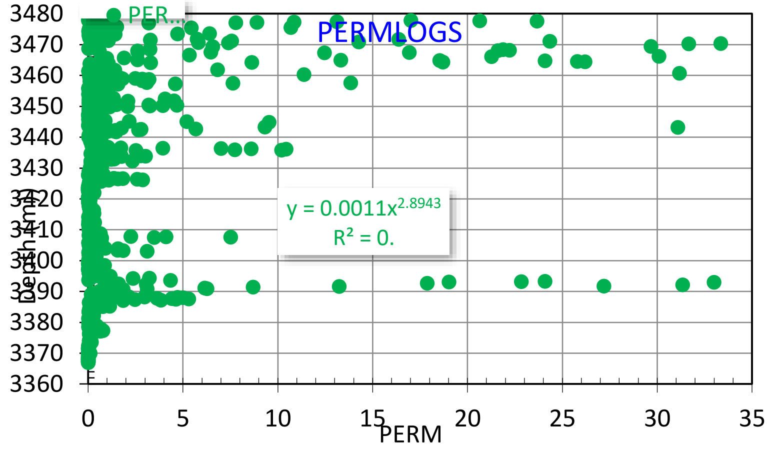

Permeability Vs Depth plot for well OMJ41

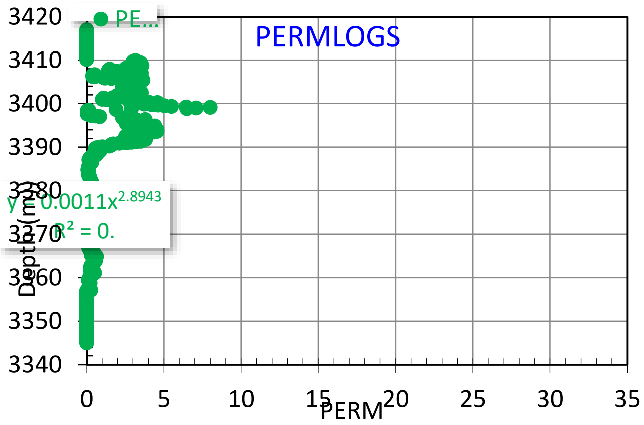

Permeability Vs Depth plot for well OMk25

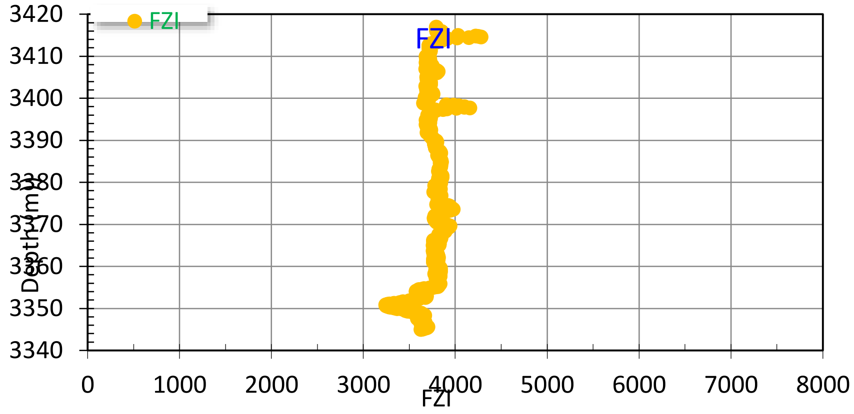

FZI vs. Depth plot for well OMk25

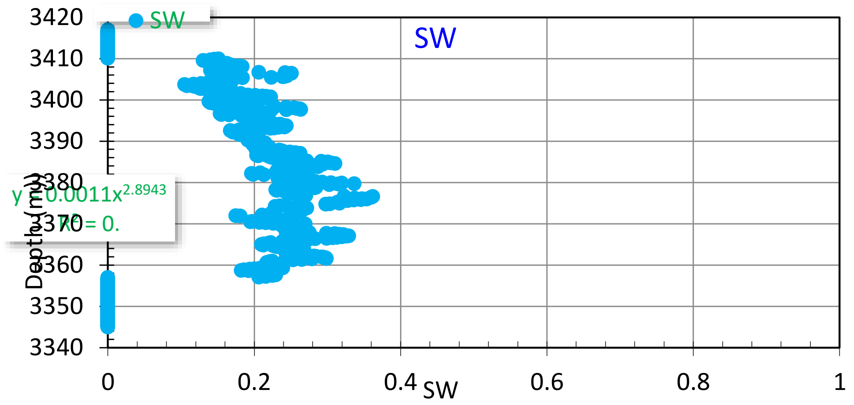

Water Saturation Vs Depth plot for well OMk25

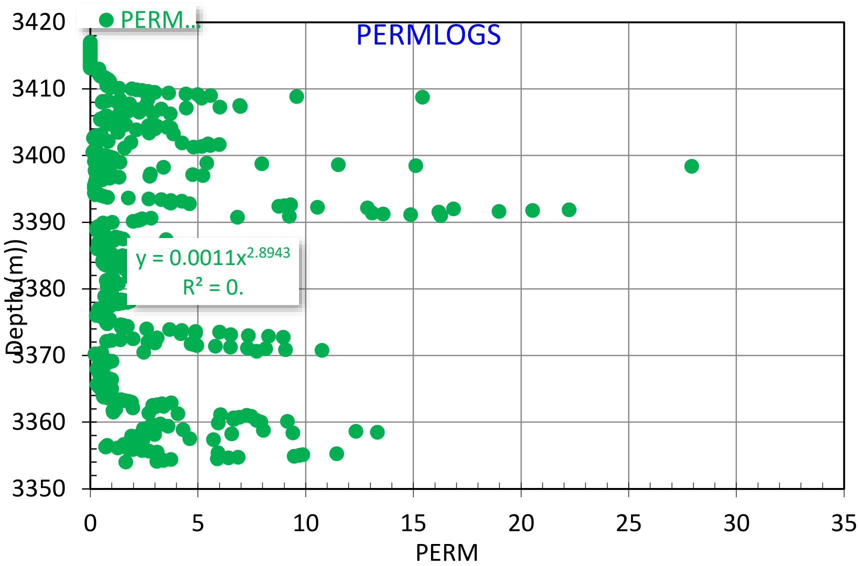

Permeability Vs Depth plot for well OMk142

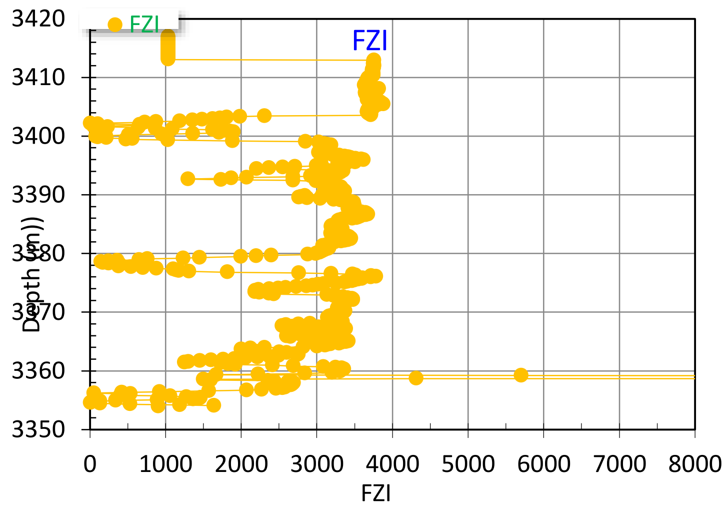

FZI vs. Depth plot for well OMk142

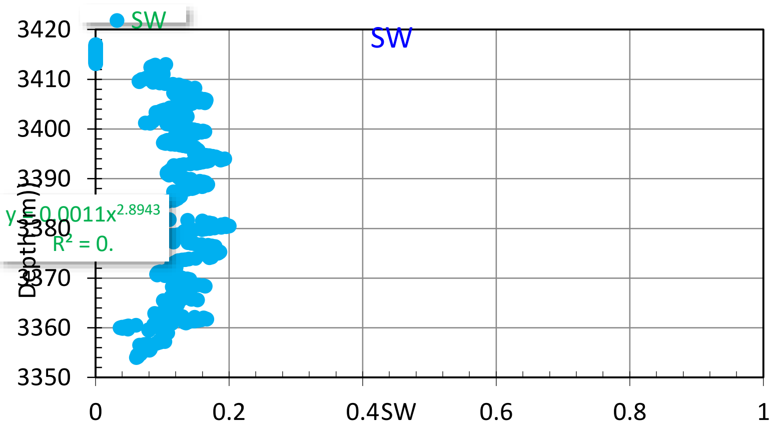

Water Saturation Vs Depth plot for well OMk142

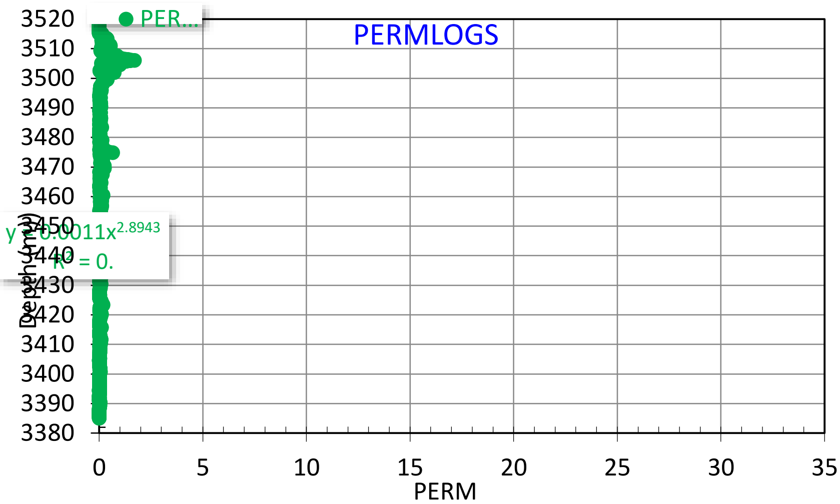

Permeability Vs Depth plot for well OMj223

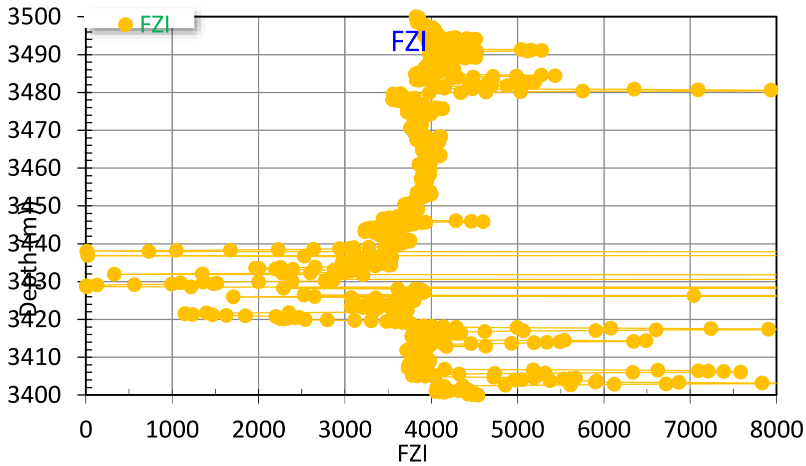

FZI vs. Depth plot for well OMj223

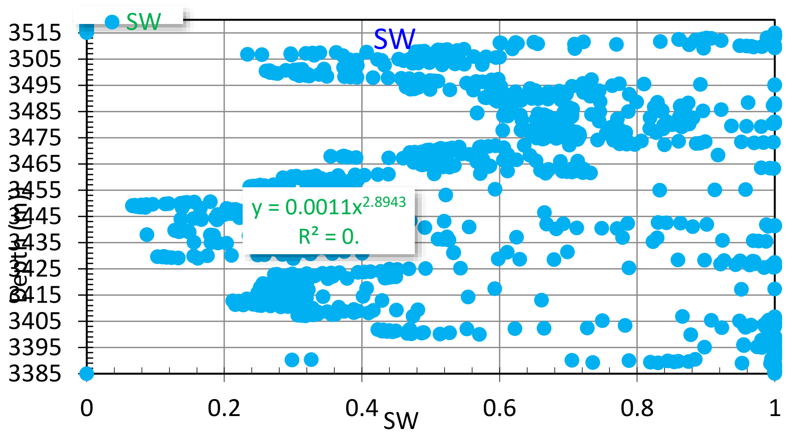

Water Saturation Vs Depth plot for well OMj223

The results revealed significant variations in reservoir rock quality among the studied wells. Well OMJ024 showed notably high FZI values exceeding 5000, indicating good effective porosity and permeability within the D5 sandstone layers. In contrast, well OMK142 exhibited strong fluctuations in FZI values, reflecting reservoir heterogeneity or increased shale content, which negatively affected hydraulic flow efficiency.

Productive zones were identified through the correlation between high FZI values and low watersaturation (SW). In well OMJ041, particularly at a depth of 3477 m, this relationship suggested the presence of hydrocarbon-bearing intervals. Moreover, well OMJ223 displayed relatively stable FZI values between 3385 and 3518 m, indicating geological homogeneity favorable for reservoir development and production.

The study concluded that FZI is an effective parameter for reservoir characterization and permeability evaluation. It also recommended periodic calibration using production logging data, along with the application of log-log permeability versus FZI plots to improve interpretation accuracy and support reservoir development decisions.

2. Microfacies Types

The sandstones of the Cambrian Ra reservoir in the northwestern part (Fig: 01), are composed essentially of mono and polycrystalline, poorly sorted, and highly compacted quartz grains. The quartz grains content reaches up to 95% in some samples of average = 73% are cemented by silica cement, sometimes with kaolinite and mica. They have medium to coarse size reaching up to 7.5 mm with an average of 2.12 mm. These sandstones are classified into some microfacies based on their cement and authigenic minerals contents. (Nassira Mebrouki, Messaoud Hacini and al, 2024)

2.1 Siliceous quartz arenite

This microfacies characterizes the D4-D3 units of the Hassi Messaoud reservoirs. It consists of poorly sorted medium to coarse-sized quartz grains (71-92 % of average 86.1 %) cemented by microcrystalline and amorphous silica cement (7-15 % of average 10. 2 %) (Fig. 4a). Some authigenic kaolinite content is also noticed (1-8 % of average 3.12 %). The quartz grains are primarily monocrystalline, and less frequently polycrystalline). The visual porosity of the present microfacies is negligible to good (3-18 % of average 12.7 %). It is primarily represented by primarily intergranular pore spaces (dyed blue, Fig. 3.2a), sometimes by micro to meso fractures and channels (Fig. 3.2b). (Nassira Mebrouki, Messaoud Hacini and al, 2024)

2.2 Kaolinitic and siliceous quartz arenite

This microfacies is commonly assigned in the Hassi Messaoud reservoirs, especially in D4 and ID units. It is primarily composed of poorly sorted very fine to pebbly-sized quartz grains (51-95 % of average 81.1 %) compacted together and cemented by microcrystalline and amorphous silica cement (3-20 % of average 8.42 %) (Fig. 3.2c). Some authigenic kaolinite content is also noticed (1-25 % of average 8.26 %) (Fig. 3.2d, e). The quartz grains are primarily monocrystalline, less frequently are polycrystalline (Fig. 3.2c, b). The visual porosity of the present microfacies is negligible to fair (1-15 % of average 3.69 %). It is represented by microporosity within the kaolinite booklets and primarily intergranular pores that are frequently highly deteriorated due to filling by patches of kaolinite booklets (Fig. 3.2d, e). As indicated by the EDAX technique, the kaolinite booklets are sometimes transformed into dickite (Fig. 3.2f, g).(Nassira Mebrouki, Messaoud Hacini and al, 2024)

2.3 Micaceous, Kaolinitic, and siliceous quartz arenite

This microfacies is presented in the various units of the Hassi Messaoud sequence, especially in the ID, D3, and D4 units. It is composed of highly compacted poorly sorted, mono to polycrystalline, and fine to coarse-grained quartz (51-92 % of an average equals 85.6 %) compacted with straight, sutured, and concavo-convex grain-to-grain contacts (Fig. 3.2h). These are cemented by microcrystalline and amorphous silica cement (7-14 % of an average equals 9.31 %) (Fig. 3.2h). Some authigenic kaolinite content (1-13 % of an average equals 6.26 %), and mica flakes (1-7 % of an average equals 4.21 %) (Fig. 3.2h) are also noticed. Traces of heavy minerals represented by zircon are also noticed (Fig. 3.2i). The mica flakes are frequently disintegrated into kaolinite (Fig. 3.2k). Also, kaolinite is sometimes alternated into illite (traces to 3 %) (Fig. 3.2l) due to the burial depth. This illite sometimes corrodes the quartz grains causing their dissolution and alteration. The visual porosity of this microfacies is negligible to fair (1-11 % of average 2.72 %). It is represented by 1) micropores within the clay patches, 2) intergranular pores that are frequently highly reduced due to filling by kaolinite booklets and illite hair-like fibers, and 3) microfractures within the quartz grains (Fig. 3.2m). The intergranular pore spaces and microfractures are sometimes filled by halite crystals with euhedral (Fig. 3.3a) to dissolved subhedral (Fig. 3.3b). (Nassira Mebrouki, Messaoud Hacini and al, 2024)

2.4 Micaceous and argillaceous subarkose

This microfacies is represented in D1, DI, and D3 units; it is composed of poorly sorted very fine to coarse-grained quartz (55-72 %), and feldspars (5-8 %) cemented by silica cement (8-13 %)

with some calcite cement (5-7 %, Fig. 3.3a), sometimes with dolomitic cement of well-developed dolomite rhombs (1-4 %) (Fig. 3.3b). This microfacies is characterized by the presence of some subhedral and euhedral halite crystals (Fig. 3.3c-e). However, it is worth mentioning that the presence of halite (NaCl) in some intervals of the W03 and W04 wells could be attributed to the contamination with salts invading from the highly saline drilling mud.

Some mica flakes are present in 2-7 %, which are squeezed between the quartz grains due to the intensive compaction of this microfacies (Fig. 3.3f-k). The argillaceous content is represented by clay patches of kaolinite, which sometimes change to illite (Fig. 3.3l, m). The porosity of this microfacies is highly deteriorated (1-5 %) due to the mica content, illitization, and compaction. Pore spaces are represented by micropores within the clay patches and micro intergranular pores.(Nassira Mebrouki, Messaoud Hacini and al, 2024)

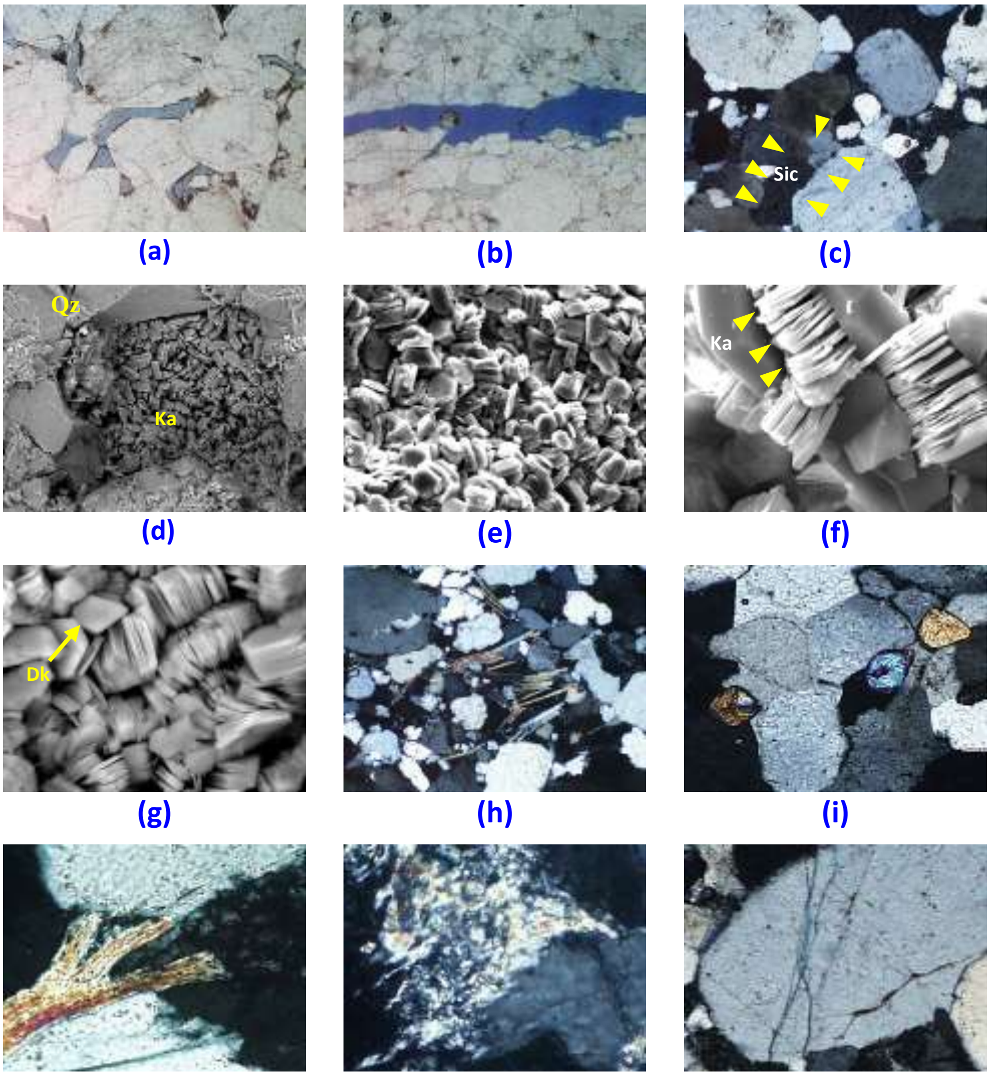

(k) (l) (m)

Fig. 3.2: Photomicorgraphs showing a) poorly sorted sandstone with some intergranular pore spaces (dyed-blue), siliceous quartz arenite microfacies, 40x, PPL, 3461.5 m depth, OMJ41 well; b) channel micro to meso fracture/pore channel due to dissolution, kaolinitic and siliceous quartz arenite microfacies, XPL, 40x, 3432 m depth, OMJ41 well; c) highly cemented and poorly sorted sandstone cemented by silica cement (Sic) with some kaolinite content (Ka), kaolinitic and siliceous quartz arenite microfacies, XPL, 40x, 3432 m depth, OMJ41 well; SEM images showing d) kaolinite bookelts filling the interstitial pore spaces, kaolinitic and siliceous quartz arenite microfacies, 343x, 3457.75 m depth, OMJ223 well; e) kaolinite bookelts filling the interstitial pore spaces, kaolinitic and siliceous quartz arenite microfacies, 661x, 3433.0 m depth, OMJ223 well; f) transformation of the kaolinite bookelts into dickite, kaolinitic and siliceous quartz arenite microfacies, 2571x, 3443.0 m depth, W03 well; g) transformation of the kaolinite bookelts into dickite (Dk), kaolinitic and siliceous quartz arenite microfacies, 1396x, 3457.75 depth, OMJ223 well, Photomicrographs showing h) mica flakes filling the intergranular pore spaces, micaceous, kaolinitic, and siliceous quartz arenite microfacies, XPL, 40x, 3474 depth, OMJ41 well, i) a few ziron mineral crystals scattered within the cement, micaceous, kaolinitic and siliceous quartz arenite microfacies, XPL, 100x, 3477.5 depth, OMJ41 well, k) transformation of kaolinite into mica, micaceous, kaolinitic and siliceous quartz arenite microfacies, XPL, 200x, 3491.5 depth, OMJ41 well, l) corrosion of the quartz grains by illite fibers, micaceous, kaolinitic and siliceous quartz arenite microfacies, XPL, 400x, 3478.5 depth, OMJ24 well, and m) microfractures within the quartz grains, micaceous, kaolinitic and siliceous quartz arenite microfacies, XPL, 100x, 3475 depth, OMJ24 well.(Nassira Mebrouki, Messaoud Hacini and al, 2024)

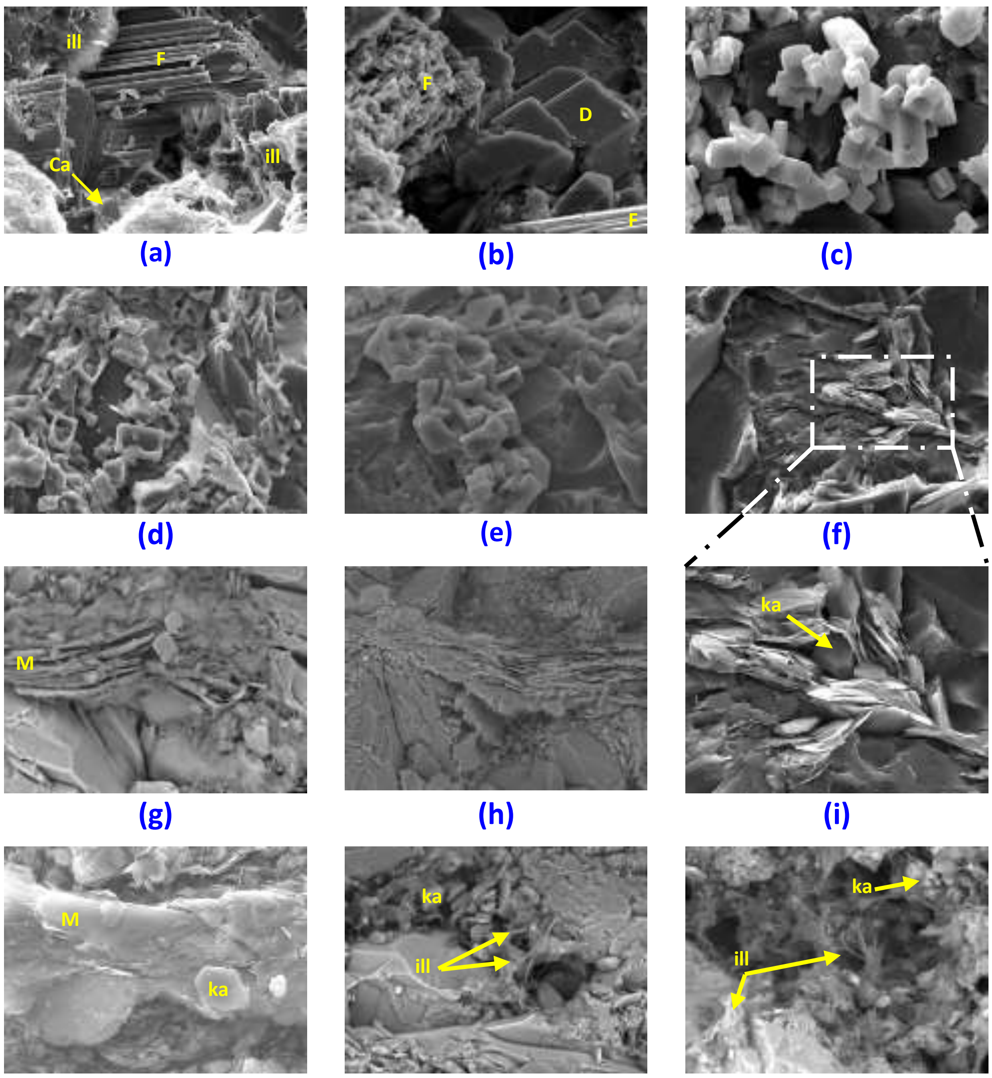

(k) **(l)** **(m)**

Fig. 3.3:SEM images showing a) feldspars (F) cemented by calcite cement (Ca) and surrounded by illite patches (ill), micaceous and argillaceous subarkose microfacies, 533x, 3380 m depth, OMK25well; b) feldspars (F) alteration of the feldspars into kaolinite. Notice the presence of some dolomite rhombs (D), micaceous and argillaceous subarkose microfacies, 1023x, 3380 m depth, OMK25 well; c) euhedral halite crystals filling the intergranular pore spaces, micaceous and argillaceous subarkose microfacies, 1600x, 3343 m depth, OMJ812 well; d) subhedral halite crystals filling the intergranular pore spaces, micaceous and argillaceous subarkose microfacies, 651x, 3396 m depth, OMJ812 well; e) subhedral halite crystals filling the intergranular pore spaces, micaceous and argillaceous subarkose microfacies, 1025x, 3369 m depth, OMJ812 well; f) mica flakes squeezed beteen the kaolinite booklets and quartz grains, micaceous and argillaceous subarkose microfacies, 872x, 3351 m depth, OMJ812 well; mica flakes in between grains of the micaceous and argillaceous subarkose microfacies in image g) 640x, 3400 m depth, OMJ812 well; and image h) 357x, 3457 m depth, OMJ223 well; i) magnification for image f indicating the kaolinite booklets, micaceous and argillaceous subarkose microfacies, 1744x, 3351 m depth, OMJ812 well; l) transformation of the kaolinite (ka) into illite (ill), micaceous and argillaceous subarkose microfacies, 640x, 3400.5 m depth, OMJ812 well; and m) illization of the kaolinite (ka) into illite (ill), micaceous and argillaceous subarkose microfacies, 725x, 3400.5 m depth, OMJ812 well. (Nassira Mebrouki, Messaoud Hacini and al, 2024)

3. Discussion

3.1 Implications of the Diagenetic Features on the Reservoir Quality

Investigating the predominant diagenetic features using the petrographic imaging of thin sections is an essential procedure to interpret the reservoir quality and delineate its main petro and pore fabric attributes. This petrographic study defines the main reservoir quality-deteriorating and supporting diagenetic features following the classification of Nabway and Kassab (2014) (Nabawy and El Aal, 2019; Nabawy et al., 2020a, b, 2023; etc..). Among these features, pressure solution and mechanical compaction, authigenic mineral content, and calcite and silica cement materials are considered reservoir quality-deteriorating features, while dissolution and fracturing are considered reservoir quality-supporting features.(Nassira Mebrouki, Messaoud Hacini and al, 2024)

3.1.1 Reservoir Quality-Deteriorating Diagenetic Features

I. Pressure solution and Mechanical Compaction

Increasing the vertical overload pressure and temperature with depth and the horizontal/inclined stresses due to the tectonic activities is among the prime eodiagenetic operations, which controlled and deteriorated the reservoir quality. The Cambrian Hassi Messaoud sandstone reservoirs have undergone a complex deteriorating history, especially due to the dominance of mechanical stresses as a main deteriorating diagenetic feature. In its intensive degree, it caused intensive packing of the quartz grains via suture contacts, which tightly compacted the grains to each other blocking all the intergranular pore spaces to cause deteriorating the pore volume (Figs. 3.3c, i, 3.4a, b), especially in the alteration zone, and sometimes in D3 and ID zones. In its mild degree, it causes bending of the mica flakes (Fig. 3.4c). On a slight implication of the mechanical compaction and pressure solution, a quartz overgrowth is noticed on the quartz grains surfaces represented by a thin dusty line surrounding the quartz grain (Fig. 3.4d, e). This deteriorating feature is responsible for reducing the reservoir quality of the PSRT5-6. However, the early kaolinitization of the studied microfacies will attenuate the compaction and pressure solution implementation.(Nassira Mebrouki, Messaoud Hacini and al, 2024)

II. Silica and Calcite Cements

In the Hassi Mesaoud reservoirs, silica is the dominant reservoir cement. Enrichment with secondary silica cement is localized to definite intervals causing high deterioration of the pore volume and reduced connectivity of the pore spaces (Figs. 3.2a, i, 3.4a, b, f). For the Hassi Messaoud reservoirs, at least two generations of secondary silica cement are assigned; it can reach up to 25 % of the bulk mineral composition with an average value equals 6.5 %. Silicification is assigned at shallow depths in the early diagenetic history due to invasion by Si-rich solutions or due to feldspars alteration causing a high reduction in the pore volume and its connectivity (Nabawy et al., 2020b). With increasing depth, the Ca-rich solutions predominate instead of the impact of the Si-rich solutions, i.e., calcite cementation predominates and supports the deteriorating implication of the Si-solutions on the reservoir quality (Figs. 3.3a, 3.4f). However, calcite cemented may be also formed at shallow depths due to the invasion of seawater. (Nassira Mebrouki, Messaoud Hacini and al, 2024)

Also, dolomite replaces the calcite partially at shallow depths in some localized intervals supporting the closure of the intergranular pore spaces of the micaceous and argillaceous subarkose microfacies (Figs. 3.3b, 6g).

III. Authigenic Mineral Content

Clay patches and iron oxides are the main authigenic minerals that are in charge of blocking the pore throats as a result of the alteration of unstable minerals like feldspars and mica flakes. Kaolinitization and illitization are the main sources of clay content for the present reservoirs based on depth during the diagenetic process. Kaolinitzation happens at relatively shallow depths due to the alteration of feldspar crystals into colonies/patches of authigenic kaolinite booklets (Figs. 3.2d, e, f, g, 3.3l, m) during high-temperature hydrothermal activities. It happens due to the disintegration of the mica flakes into kaolinite booklets (Fig. 3.4k). This process caused an increase in the authigenic kaolinite content instead of mica; however, both are deteriorating factors for the reservoir quality. Kaolinitization happens at higher K+/H+ activity ratio and temperatures than dickitization where dickite is present at a relatively low K+/H+ activity ratio (Lanson et al., 2002). Dickite is present because with increasing the burial depth and temperature, kaolinite tends to stabilize itself by transforming into more resistant and stable minerals like dickite and generating a new form of silica cement. However, the dickitization process is presented locally at some intervals of the kaolinitic and siliceous quartz arenite microfacies (Fig. 3.4f, g).(Nassira Mebrouki, Messaoud Hacini and al, 2024)

The large amount of illite in the area reflects the high K^+/H^+ ratio in the diagenetic system, so the amount of dickite in the sandstones must be limited. The presence of some illite patches (Fig. 3.3a, l, m) in the Hassi Messaoud reservoirs reflects a relatively high K^+/H^+ causing high deterioration of the pore spaces by trapping the fine migrating particles due to its hair-like structure (Fig. 3.4l, m). The illitization process predominates at deeper depths than the kaolinite mineral, which changes to illite by increasing depth. (Nassira Mebrouki, Messaoud Hacini and al, 2024)

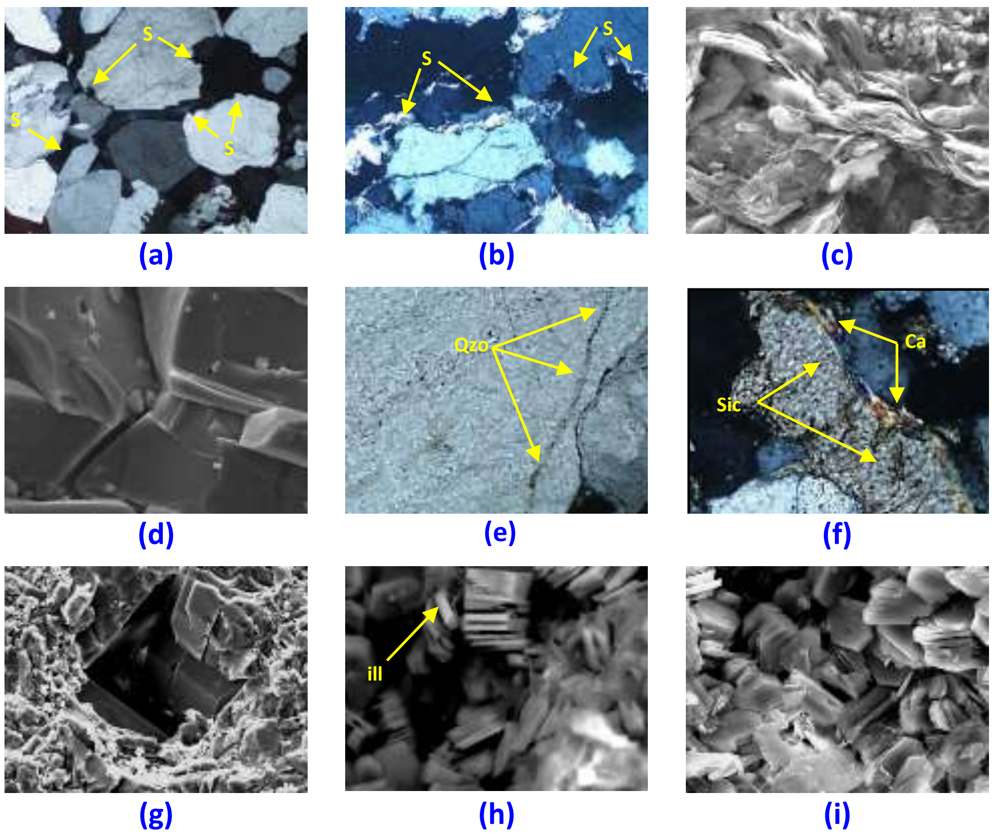

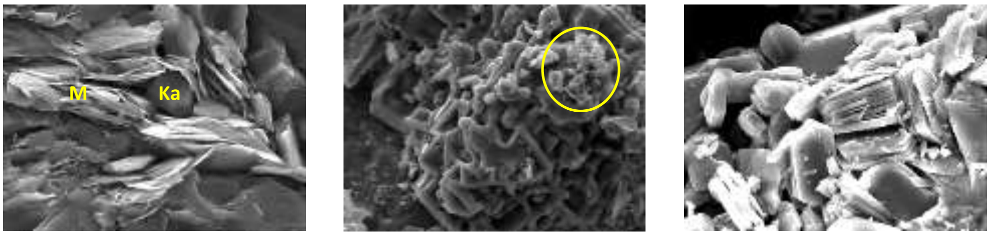

(k) (l) (m)

Fig. 3.4: Photmicrographs presenting the tight compaction causing the suture grain-to-grain contacts (S) between the quartz grains and diminishing the intergranular porespace network patterns of the micaceous, kaolinitic and siliceous quartz arenite microfacies, 40x, 3461.5 m depth, OMJ41 well (a), and the kaolinitic and siliceous quartz arenite microfacies, 100x, 3473 m depth, OMJ41well (b). SEM images showing c) bended mica flakes between the quartz grains due to mild stresses, micaceous and argillaceous subarkose microfacies, 1804x, 3424 m depth, OMJ223 well; and d) quartz overgrowth, micaceous and argillaceous subarkose microfacies, 1051x, 3369 m depth, OMJ812 well. Photomicrographs showing e) the quartz overgrowth (Qzo), siliceous quartz arenite micorfacies, 100x, XPL, 3486 m depth, OMJ24 well; and f) secondary silica cement (Sic) filling the pore spaces with a few calcite patches (Ca), micaceous and argillaceous subarkose, 200x, PPL, 3449 m depth, OMJ24 well. SEM images showing g) filling the intergranular pore spaces with well-developed euhedral dolomite rhombs, micaceous and argillaceous subarkose microfacies, 450x, 3380 m depth, OMK25 well; h) kaolinitization and illitization (ill) filling the intergranular pore spaces, micaceous, kaolinitic and siliceous quartz arenite microfacies, 1523x, 3457.8 m depth, OMJ223well; i) transformation of kaolinite into dikite crystallined in pseudo hexagonal forms, micaceous, kaolinitic and siliceous quartz arenite microfacies, 1325x, 3401.0 m depth, W06 well; k) filling the pore spaces due to kaolinitzation of the mica flakes, micaceous, kaolinitic and siliceous quartz arenite microfacies, 1744x, 3351.5 m depth, OMJ812 well; l) illitization process filling the pore spaces, kaolinitic siliceous quartz arenite microfacies, 800x, 3343 m depth, OMJ812 well; and m) transformation of the kaolinite booklets into hair like illite patches, kaolinitic siliceous quartz arenite microfacies, 1322x, 3443 m depth, OMJ41 well.(Nassira Mebrouki, Messaoud Hacini and al, 2024)

4.1.2 Reservoir Quality-supporting Diagenetic Factors

I. Fracturing

Cement and grain fracturing are among the secondary diagenetic features that support the reservoir quality. It is caused due to increasing the overload pressure with depth acting on the quartz grains to create some internal fractures (Fig. 3.2m). It is also caused due to increasing the tectonic activities that controlled the Hassi Messaoud reservoirs by the end of the deposition of the Ra reservoir. These tectonic activities were the prime cause of creating a set of fractures acting through the cement of the kaolinitic and siliceous quartz arenite microfacies. The created fractures are the main weakness entrances for invading the solutions to modify them into channels and vuggy channels (Fig. 3.2b).(Nassira Mebrouki, Messaoud Hacini and al, 2024)

II. Dissolution

In the early diagenetic phases of the Hassi Messaoud reservoirs, dissolution of unstable silicate minerals like the feldsp**3**ars prevails liberating the k, Al, and Si cations to form secondary silica and kaolinite. Dissolution and leaching of these unstable minerals are the main factors supporting the reservoir quality by creating additional secondary intergranular and intercrystalline pores (Figs. 3.2a, 3.3b, c, 3.4g, h), channels (Fig. 3.2b), and vugs in particular for the siliceous quartz arenite and the kaolinitic and siliceous quartz arenitemicrofacies.(Nassira Mebrouki, Messaoud Hacini and al, 2024)

Conclusion

-Petrographically, the high petrophysical heterogeneity observed in the Cambrian Hassi Messaoud reservoirs is attributed to their mineral composition and complex architecture.

- These reservoir sequences predominantly consist of poorly sorted sandstones comprising siliceous, micaceous, kaolinitic, and calcareous quartz arenites and arkoses.
- Fracturing and dissolution pla
- y significant roles in improving reservoir quality, while physical compaction and the presence of silica, kaolinite, mica, and calcite cements contribute to deteriorating reservoir quality.

- FZI,the use of well data for calculating (FZI) proved to be an effective approach for reservoir characterization and permeability evaluation in uncored intervals. FZI values and permeability variations were identified in both productive and non-productive reservoir zones. High FZI values observed in well OMJ024 indicated good reservoir quality with enhanced porosity and permeability within the D5 sandstone layers, whereas fluctuating FZI values in well OMK142 reflected reservoir heterogeneity and increased shale content, leading to reduced hydraulic flow efficiency. The correlation between high FZI values and low water saturation (SW) successfully identified hydrocarbon-bearing intervals, particularly in well OMJ041 at a depth of 3477 m. In addition, the relatively stable FZI values recorded in well OMJ223 between 3385 and 3518 m suggested geological homogeneity favorable for reservoir development and production. The study demonstrates that FZI is a reliable parameter for identifying Hydraulic Flow Units (HFUs) and improving reservoir evaluation, while periodic calibration with production logging data can further enhance interpretation accuracy and reservoir management decisions.

References

Abdeen, M.M., Ramadan, F.S., Nabawy, B.S., El Saadawy, O., 2021. Subsurface structural setting and hydrocarbon potentiality of the Komombo and Nuqra basins, south Egypt: a seismic and petrophysical integrated study. Nat. Resour. Res. 30 (5), 3575-3603.

Abuamarah, B.A., Nabawy, B.S., 2021. A proposed classification for the reservoir quality assessment of hydrocarbon-bearing sandstone and carbonate reservoirs: a correlative study based on different assessment petrophysical procedures. J. Nat. Gas Sci. Eng. 88, 103807.

Abuhagaza, A.A., El Sawy, M.Z., Nabawy, B.S., 2021. Integrated petrophysical and petrographical studies for characterization of reservoirs: a case study of Muglad Basin, North Sudan. Environmental Earth Sciences 80(5), 171

Aïfa, T., Zerrouki, A.A., Baddari, K., Géraud, Y., 2014. Magnetic susceptibility and its relation with fractures and petrophysical parameters in the tight sand oil reservoir of Hamra quartzites, southwest of the Hassi Messaoud oil field, Algeria Journal of Petroleum Science and Engineering 123, 120-137.

Ali, O., 1975. El Agreb-El Gassi Oil Fields, Central Algerian Sahara: Geologic Notes. *AAPG Bulletin*, 59(9), 1676-1684.

Amaefule, J., Altunbay, M., Tiab, D., Kersey, D., Keelan, D., 1993. Enhanced reservoir description using core and log data to identify hydraulic flow units and predict permeability in uncored intervals/wells. SPE 26436, 205-220.

Ashoor, R., Nabawy, B.S., Kamel, A., 2023. Formation evaluation and reservoir quality assessment of the Albian clastic sequence in the SWM Oilfield, Southwest the Mesopotamian Basin, Iraq. J. Pet. Explor. Prod. Technol. 13, 553-576.

Balducchi, A., Pommier, G., 1970. Cambrian Oil Field of Hassi Messaoud, Algeria, in Halbouty, M.T., ed., Geology of giant Petroleum Fields: AAPG Memoir no. 14, p. 477-488.

Baouche, R., Nabawy, B.S., 2021. Permeability prediction in argillaceous sandstone reservoirs using fuzzy logic analysis: A case study of Triassic sequences, Southern Hassi R'Mel Gas Field, Algeria. Journal of African Earth Sciences 173, 104049.

Bacheller, W.D., Peterson, R.M., 1991. Hassi Messaoud Field, Algeria; Trias Basin, Eastern Sahara Desert. In: Foster, N.H., et al. (eds) Structural Traps V, American Association of Petroleum Geologists, Treatise of Petroleum Geology, Atlas of Oil and Gas Fields, 211-225.

Benayad, S., Ysbaa, S., Chaouchi, R., Haddouche, O., Kacimi, A., 2019. Sedimentological characteristics and reservoir quality prediction in the Upper Ordovician glaciogenic sandstone of the In-Adaoui-Ohanet gas field, Illizi basin, Algeria. J. Petrol. Sci. Eng., 179, 159-172.

Bessa, F., 2004. Reservoir characterization and reservoir modeling in the northwestern part of Hassi Messaoud Field, Algeria. PhD Thesis, Hamburg, Germany, 98p.

Beuf, S., Biju-Duval, B, DE Charpal, O., Rognon, P., Gariel, O., Bennacef, A., 1971. Les Grés du Paléozoique Inférieur au Sahara. Editions Technip, Paris. Publications de l'Institut Français du Pétrole, Science et Technique du Pétrole, 18, 464.

Boote, D.R.D., Clark-Lowes, D.D., Traut, M.W., 1998. Palaeozoic petroleum systems of North Africa. In: Macgregor, D.S., Moody, R.T.J., & Clark-Lowes, D.D. (eds) 1998. Petroleum Geology of North Africa. Geological Society, London, Special Publication no. 132, 7-68.

Boutoutaou, Dj., 2003. Understanding the Regional Migration Routes and Field Charging History of the Oued Mya-Hassi Messaoud Petroleum System, Algeria. PhD Dissertation, University of Newcastle upon Tyne, U.K., 411p.

Cherana, A., Aliouane, L., Doghmane, M.Z., Ouadfeul, S.A., Nabawy, B.S., 2022. Lithofacies discrimination of the Ordovician unconventional gas-bearing tight sandstone reservoirs using a subtractive fuzzy clustering algorithm applied on the well log data: Illizi Basin, the Algerian Sahara. Journal of African Earth Sciences196, 104732

David, C., Bertauld, D., Dautriat, J., Sarout, J., Menéndez, B., Nabawy, B., 2015. Detection of moving capillary front in porous rocks using X-ray and ultrasonic methods. Frontiers in Physics 3, 1-14. A053.

Dvorkin, J., Mavko, G., 2005. P-Wave Attenuation in Reservoir and Non-Reservoir Rock. Conference: 67th EAGE Conference & Exhibition.

El Aal, A.A., Nabawy, B.S., 2019. Implications of increasing the ferruginous cement on the physical and mechanical properties of the Cambro-Ordovician Wajid Sandstone in southwest Saudi Arabia: applications for construction purposes. Bulletin of Engineering Geology and the Environment 78(2), 817-836

Elmahdy, M., Radwan, A.A., Nabawy, B.S., Abdelmaksoud, A., Nastavkin, A.V., 2023. Integrated geophysical, petrophysical and petrographical characterization of the carbonate and clastic reservoirs of the Waihapa Field, Taranaki Basin, New Zealand. Marine and Petroleum Geology 151, 106173

English, K.L., Redfern, J., Dermot, C.V., English, J.M., Cherif, R.Y., 2016. Constraining burial history and petroleum charge in exhumed basins: new insights from the Illizi Basin, Algeria. Am. Assoc. Pet. Geol. Bull., 4 (4), 623-655.

Fallah-Bagtash, R., Adabi, M.H., Nabawy, B.S., Omidpour, A., Sadeghi, A., 2022. Integrated petrophysical and microfacies analyses for a reservoir quality assessment of the Asmari Dolostone sequence in the Khesht Field, SW Iran. J. Asian Earth Sci. 223, 104989.

Fea, I., Abioui, M., Nabawy, B.S., Jain, S., Bruno, D.Z., Kassem, A.A., Benssaou, M., 2022. Reservoir quality discrimination of the Albian-Cenomanian reservoir sequences in the Ivorian basin: a lithological and petrophysical study. Geomechanics and Geophysics for Geo-Energy and Geo-Resources 8(1), 1.

Galeazzi, S., Point, O., Haddadi, N., Mather, J., Druesne, D., 2010. Regional geology and petroleum systems of the Illizi – Berkine area of the Algerian Saharan Platform : an overview. Mar. Petrol. Geol., 27 (1), 143-178.

Haque, A.E., Qadri, S.M.T., Bhuiyan, M.A.H., Navid, M., Nabawy, B.S.,,Hakimi, M.H., Abd-El-Aal, A.K., 2022..Integrated wireline log and seismic attribute analysis for the reservoir evaluation: A case study of the Mount Messenger Formation in Kaimiro Field, Taranaki Basin, New Zealand. Journal of Natural Gas Science and Engineering 99, 104452

Kassem, A.A., Osman, O.A., Nabawy, B.S., Baghdady, A.R., Shehata, A.A., 2022. Microfacies analysis and reservoir discrimination of channelized carbonate platform systems: an example from the Turonian Wata Formation, Gulf of Suez, Egypt. J. Petrol. Sci. Eng. 212, 110272.

Klett, T.R., 2000. Total petroleum systems of the Illizi province, Algeria and Libya-Tanezzuft-Illizi. U.S. Geol. Surv. Bull. 2202–A, version 1 (iii), pp. 1-76

Kurniawan, D.H., Winardi, S., Anggara, F., 2021. Linking Between Sedimentary Facies and Petrophysical Rock Type: A Case Study. IOP Conference Series: Earth and Environmental Science, v 789, International Conference on the Ocean and Earth Sciences 18-20 November 2020, Jakarta Selatan, Indonesia.

Lai, J., Wang, S., Zhang, C., Wang, G., Song, Q., Chen, X., Yang, K., Yuan, C., 2020. Spectrum of pore types and networks in the deep cambrian to lower ordovician dolostones in tarim basin, China. Mar. Petrol. Geol. 112, 104081.

Lanson, B., Beaufort, D., Berger, G., Bauer, A., Cassagnabère, A., Meunier, A., 2002. Authigenic kaolin and illitic minerals during burial diagenesis of sandstones: A review. Clay Minerals, 37(1), 1-22. doi:10.1180/0009855023710014

Malenfer, J., Tillous, A., 1963. Study of the Hassi Messaoud Field stratigraphy, structural aspect, study of detail of the reservoir: IFB review, 18, 851-867 (in French).

Nabawy, B.S., 2018. Impacts of fossil anisotropy on the electric and permeability anisotropy of highly fossiliferous limestone: a case study. Mar. Geophys. Res. 39 (4), 537-550.

Nabawy, B.S., El Aal, A.A., 2019. Impacts of the petrophysical and diagenetic aspects on the geomechanical properties of the dolomitic sequence of Gebel El-Halal, Sinai, Egypt. Bulletin of Engineering Geology and the Environment 78(4), 2627-2640.

Nabawy, B.S., El Sharawy, M.S., 2018. Reservoir assessment and quality discrimination of Kareem Formation using integrated petrophysical data, Southern Gulf of Suez, Egypt. Marine and Petroleum Geology 93, 230-246.

Nabawy, B.S., Shehata, A.M., 2015. Integrated petrophysical and geological characterization for the Sidi Salem-Wakar sandstones, off-shore Nile delta, Egypt. J. Afr. Earth Sci. 110, 160-175.

Nabawy, B.S., Wassif, N.A., 2017. Effect of the mineralogical composition on the petrophysical behavior of the amygdaloidal and vesicular basalt of Wadi Wizr, Eastern Desert, Egypt. J. Afr. Earth Sci. 134, 613-625.

Nabawy, B.S., El-Bialy, M., Hamimi, Z., Khamis, H.A., Abdel Wahed, S.A., Osman, R.A., Afify, A.M., 2023. Implication of the diagenetic evolution, litho- and microfacies types on the storage capacity of the carbonate rocks in West Esh El Mallaha area, SW onshore Gulf of Suez, Egypt. Journal of African Earth Sciences 204, 104971.

Nabawy, B.S., Khalil, H.M., Fathy, M.S., Ali, F., 2020a. Impacts of microfacies type on reservoir quality and pore fabric anisotropy of the Nubia sandstone in the central Eastern Desert, Egypt. Geol. J. 55 (6), 450-4524.

Nabawy, B.S., Mansour, A.S., Rashed, M.A., Afify, W.S.M., 2020b. Implementation of sedimentary facies and diagenesis on the reservoir quality of the Aquitanian-

Burdigalian Rudeis Formation in the Gulf of Suez, Egypt: a comparative surface and subsurface study. Geol. J. 55 (6), 4543–4563.

Nabawy, B.S., Lashin, A.A., Barakat, M.K., 2022a. Implementation of lithofacies and microfacies types on reservoir quality and heterogeneity of the late cretaceous Upper Bahariya member in the Shurouk Field, Shoushan basin, North Western desert, Egypt. J. Asian Earth Sci. 224, 105014.

Nabawy, B.S., Abudeif, A.M., Masoud, M.M., Radwan, A.E., 2022b. An integrated workflow for petrophysical characterization, microfacies analysis, and diagenetic attributes of the Lower Jurassic type section in northeastern Africa margin: Implications for subsurface gas prospection. Marine and Petroleum Geology 140, 105678

Nabawy, B.S., Mostafa, A., Radwan, A.A., Kotb, A.G., Leila, M., 2023. Seismic reservoir characterization of the syn-rift lower Miocene Rudeis Formation in the July oilfield, Gulf of Suez basin, Egypt: Implication for reservoir quality assessment. Geoenergy Science and Engineering 226, 211797

Nabway, B.S., Kassab, M.A., 2014. Porosity-reducing and porosity-enhancing diagenetic factors for some carbonate microfacies: a guide for petrophysical facies discrimination. Arabian Journal of Geosciences 7(11), 4523-4539.

Nassira Mebrouki, Messaoud Hacini, Bassem Nabawy , Mohamed I. Abdel-Fattah, 2024.Deciphering the implication of microfacies types and diagenesis on the reservoir quality of the Cambrian sequence in Hassi Messaoud Field, Algeria. Marine and Petroleum Geology

Radwan, A.A., Nabawy, B.S., 2022. Hydrocarbon prospectivity of the miocene-pliocene clastic reservoirs, Northern Taranaki basin, New Zealand: integration of petrographic and geophysical studies. Journal of Petroleum Exploration and Production Technology 12(7), 1945-1962.

Radwan, A.A., Nabawy, B.S., Abdelmaksoud, A., Lashin, A., 2021. Integrated sedimentological and petrophysical characterization for clastic reservoirs: A case study from New Zealand. Journal of Natural Gas Science and Engineering 88, 103797

Radwan, A.A., Nabawy, B.S., Shihata, M., Leila, M., 2022a. Seismic interpretation, reservoir characterization, gas origin and entrapment of the Miocene-Pliocene Mangaa C sandstone, Karewa Gas Field, North Taranaki Basin, New Zealand. Marine and Petroleum Geology 135, 105420

Radwan, A.A., Abdelwahhab, M.A., Nabawy, B.S., Mahfouz, K.H., Ahmed, M.S., 2022b. Facies analysis-constrained geophysical 3D-static reservoir modeling of Cenomanian units in the Aghar Oilfield (Western Desert, Egypt): Insights into paleoenvironment and petroleum geology of fluviomarine systems. Marine and Petroleum Geology 136, 105436

Radwan, A.A., Nabawy, B.S., Kassem, A.A., Elmahdy, M., 2023. An integrated workflow for seismic interpretation, petrophysical and petrographical characterization for the clastic Mangahewa reservoir in Pohokura gas field, Taranaki Basin, New Zealand. Geoenergy Science and Engineering 229, 212117

Safa, M.G., Nabawy, B.S., Basal, A.M.K., Omran, M.A., Lashin, A., 2021. Implementation of a petrographical and petrophysical workflow protocol for studying the impact of heterogeneity on the rock typing and reservoir quality of reefal limestone: a case study on the nullipore carbonates in the Gulf of Suez. Acta Geol. Sin. 95 (5), 1746-1762.

Shehata, A.A., Osman, O.A., Nabawy, B.S., 2021. Neural network application to petrophysical and lithofacies analysis based on multi-scale data: an integrated study using conventional well log, core and borehole image data. J. Nat. Gas Sci. Eng. 93, 104015.

Shenawi, S.H., White, J.P., Elrafie, E.A., Kilany, K.A., 2007. Permeability and water saturation distribution by lithologic facies and hydraulic units: a reservoir simulation case study: society of petroleum engineers. In: 15th Society of Petroleum Engineers Middle East Oil & Gas Show and Conference, Kingdom of Bahrain. Paper no. 105273.

Teama, M.A., Nabawy, B.S., 2016. Petrophysical evaluation of the hydrocarbon potential of the Lower Cretaceous Kharita clastics, North Qarun oil field, Western Desert, Egypt. Journal of African Earth Sciences 121, 62-71.

Tempre, C., Claret, J., 1967. Une Nouvelle Région Productrice au Sahara Algérien: l'Anticlinorium d'Hassi Touareg. 7th World Petroleum Congress, Mexico City, Mexico, April 1967, WPC-12108.

WEC, 2007. Hydrocarbon Reservoirs of Algeria. Sonatrach internal report.

Winland, H.D., 1972. Oil accumulation in response to pore size changes. Weyburn Field, Saskatchewan. Amoco Production Research Report No. F72-G-25 197.

Zerroug, S., Bounoua, N., Lounissi, R., Zeghouani, R., Djellas, N., Kartobi, K., Etchecopar, A., Mohamed Tchambaz, M., Abadir, S., Simon, P., Fuller, J. (2007). Well Evaluation Conference Algeria (WEC), Published by Schlumberger, Produced by Lynx Consulting, Inc., Houston, TX, USA, 489 pp.